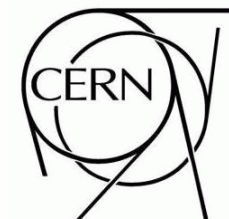




ATLAS NOTE

ATL-COM-PHYS-2010-695



Single Boson and Diboson Production Cross Sections in pp Collisions at $\sqrt{s} = 7$ TeV

J.M. Butterworth¹, E. Dobson², U. Klein³, B.R. Mellado Garcia⁴,
T. Nunnemann⁵, J. Qian⁶, D. Rebuzzi⁷, and R. Tanaka⁸

¹ *University College London, London WC1E 6BT, United Kingdom*

² *Oxford University, Oxford OX1 3RH, United Kingdom*

³ *University of Liverpool, Oliver Lodge Laboratory, Liverpool L69 3BX, United Kingdom*

⁴ *University of Wisconsin, Madison, Wisconsin 53706, USA*

⁵ *Ludwig-Maximilians-Universität München, DE-86748 Garching, Germany*

⁶ *University of Michigan, Ann Arbor, Michigan 48109, USA*

⁷ *Università di Pavia and INFN Sezione di Pavia, IT-27100 Pavia, Italy and*

⁸ *LAL, Univ. Paris-Sud, IN2P3/CNRS, Orsay, France*

(Dated: October 27, 2010)

Total inclusive cross sections of single boson (W or Z) and diboson (WW , WZ or ZZ) production in pp collisions at a center-of-mass energy $\sqrt{s} = 7$ TeV are presented. QCD corrections are calculated up to next-next-leading order for W and Z productions and to next-leading order for diboson productions. Cross section uncertainties are estimated for missing higher order corrections, uncertainties of parton density functions and strong coupling constant value. Cross sections for other \sqrt{s} values of both pp and $p\bar{p}$ collisions are also included.

I. INTRODUCTION

The LHC is expected to operate at $\sqrt{s} = 7$ TeV to accumulate an integrated luminosity of $\sim 1 \text{ fb}^{-1}$ by the end of 2011. Many standard model measurements and searches for new physics beyond the standard model will be made at this energy. Cross sections of well known standard model processes such as single and diboson productions are therefore important for these measurements and searches. This note documents a recent study of single boson and diboson production cross sections in pp collisions at $\sqrt{s} = 7$ TeV using latest available theoretical tools. In anticipation of comparisons with previous measurements and the future increase of the LHC collision energy, we have also included cross sections of both pp and $p\bar{p}$ collisions at other values of \sqrt{s} . The note is intended as a supporting note to the ATLAS standard model cross section task force report and the recent ATLAS CONF notes [1]. Some previous cross-section calculations/compilations of standard model processes can be found in Ref. [2].

A. Theoretical Calculations and Programs

In the following document, single and diboson production cross section at LHC have been estimated up to next-to-next-to-leading order (NNLO) for single bosons, and up to next-to-leading order (NLO) for dibosons in QCD perturbative expansion. These calculations have been implemented in several programs. Those used in this study are:

- **MC@NLO**

MC@NLO [3] is a Fortran package which combines a Monte Carlo event generator with NLO calculations for QCD processes. MC@NLO makes use of the Fortran HERWIG event generator [4] for the parton shower and hadronization/fragmentation processes, but in the present note, only its predictions on inclusive cross sections have been considered, with no event generation. The latest version 3.41, release on October 2009 has been used.

- **MCFM**

MCFM [5] is a parton-level Monte Carlo program which gives cross section predictions for a large number processes at hadron colliders. In particular, it calculates single and diboson production cross sections at LO and NLO in QCD perturbation expansion. We use version 5.8.

- **FEWZ**

The Fortran codes FEWZw and FEWZz [6] (collectively referred as FEWZ below) compute the production cross sections of W and Z bosons at hadron collisions up to NNLO in perturbative QCD. The programs include leptonic decays of W and Z bosons with full spin correlations and finite width effects and $Z(\gamma^*)$ interference. It allows selections based on final-state kinematics. However, the NNLO calculation is notoriously slow to get a good integration precision. Nevertheless, the integration precision is on the order of or better than 0.1% for all the cross sections calculated using FEWZ quoted in this note.

- **ZWPROD**

ZWPROD(MS) calculates the total inclusive production cross section for Z and W boson production cross section up to NNLO QCD [7]. For Z and W bosons, the calculation is performed using the zero-width approximation, i.e. boson decays and photon exchange are not considered. The cross sections presented in this note were obtained using the version of the code dated 2002 with additional private modifications. We added numerous additional PDF sets, an interface to LHAPDF [8], and the NNLO evolution for α_s and increased the precision of the integration to obtain negligible statistical uncertainties. For Z boson, terms which include b or \bar{b} quarks in the initial state were added. For W boson production we neglected these terms due to the small value of V_{cb} . Since no W and Z decays are involved, the programs are fast to run and are valuable tools for quick studies and for estimating theoretical uncertainties.

- **gg2WW and gg2ZZ**

The programs gg2WW [9] and gg2ZZ [10] implements a complete calculation of gluon-induced loop processes $gg \rightarrow Z(\gamma^*)Z(\gamma^*) \rightarrow 4\ell$ and $gg \rightarrow WW \rightarrow \ell\nu\ell'\nu$, respectively. They contribute to WW and ZZ productions in pp collisions at NNLO and therefore are not included in the NLO calculations of $q\bar{q}$ -induced processes implemented in programs such as MCFM and MC@NLO. Their contributions need to be evaluated separately.

B. Input Parameters

The standard model input parameter values are chosen to follow the recommendation of the ATLAS standard model cross section task force, as summarized in Table I. They are similar to those used for the ATLAS MC09 production [11]

and are PDG averages a few year ago [12]. Since most of the calculations discussed below are at leading-order in electroweak corrections, the electromagnetic coupling constant $\alpha(M_Z)$ and weak mixing angle $\sin^2 \theta_W$ are set to their derived values from M_W , M_Z and G_F in the so-called G_μ scheme

$$\frac{1}{\alpha_G} = \frac{\sqrt{2}G_\mu M_W^2}{\pi} \left(1 - \frac{M_W^2}{M_Z^2} \right); \quad \sin^2 \theta_W = 1 - \frac{M_W^2}{M_Z^2}$$

to minimize higher order electroweak corrections. Partial $W \rightarrow \ell\nu$ and $Z \rightarrow \ell\ell$ decay widths are required as inputs to some programs (e.g. FEWZ) and they are taken to be the standard model predicted values.

| | | | |
|----------------------------------|---|----------|-----------|
| M_W | 80.403 GeV | V_{ud} | 0.9738 |
| Γ_W | 2.0910 GeV | V_{us} | 0.2272 |
| $\Gamma(W \rightarrow \ell\nu)$ | 0.22629 GeV | V_{ub} | 0.0040 |
| M_Z | 91.1876 GeV | V_{cd} | 0.2271 |
| Γ_Z | 2.4952 GeV | V_{cs} | 0.9730 |
| $\Gamma(Z \rightarrow \ell\ell)$ | 0.08398 GeV | V_{cb} | 0.0422 |
| $1/\alpha_G$ | 132.34 | V_{td} | 0.0081 |
| $\sin^2 \theta_W$ | 0.22255 | V_{ts} | 0.0416 |
| G_F | $1.16637 \times 10^{-5} \text{ GeV}^{-2}$ | V_{tb} | 0.9991 |
| N_F | 5 | m_c | 1.29 GeV |
| m_{ud} | 0.32 GeV | m_b | 4.2 GeV |
| m_s | 0.50 GeV | m_t | 172.5 GeV |

TABLE I: Set of input parameters used for the evaluation of the single and diboson cross sections.

The values of the strong coupling constant α_s at the scale of Z boson mass are generally taken from the parton density function set used, as discussed in the following paragraph.

C. Parton Density Functions

All the above-mentioned programs implement LHAPDF accords or provide interfaces to the two popular CTEQ and MSTW families of parton density functions (PDF) in their software distributions. Thus for the calculations below, CTEQ and MSTW PDF sets are used extensively.

- **CTEQ PDFs: CTEQ6.6, CT10 and CT10W**

The CTEQ6.6 [13] is a NLO parton distributions, obtained by global analysis of hard scattering data in the framework of general-mass perturbative QCD, consist of a central PDF set and 44 eigenvector error sets at 90% confidence level (CL) that span the range of uncertainties in the parton parameter space due to input experimental uncertainties. The evolution equation from the low energy region to the high energy range is performed at NLO. The CTEQ6.6 PDFs are based on an implementation of the heavy-quark mass effect in perturbative QCD cross sections, which leads to significant changes in some key predictions, with respect to the ordinary zero-mass scheme. The quality of the global analysis is further enhanced by the inclusion of newer data sets, relaxation of *ad hoc* constraints on the parameterization of strange quark PDFs, and improvements in the global fitting procedure.

The CTEQ6.6 PDFs are superseded by the recently published CT10 and CT10W PDF sets [14]. Additional experimental data sets were included in the fit: combined HERA-I DIS data, Tevatron inclusive jet production and measurements of Z -rapidity and W -asymmetry. Modifications in the theoretical treatment include a common weight for all data sets and a more flexible parametrization for the d , s , g PDFs which increases the s and g PDF uncertainties in some kinematic region despite the inclusion of additional data sets. As D0's Run II measurements of the charge asymmetry in W events, while being very precise, exhibit tension with themselves and other data sets, they are excluded in the CT10, but included (with increased weight) in the CT10W PDF set. For both CT10 and CT10W, 52 eigenvector error sets and PDF sets for varied strong coupling α_s are published.

- **MSTW2008**

MSTW2008 [15] parton distribution functions, determined from global analysis of hard scattering data within the standard framework of leading-twist fixed-order collinear factorization in the \overline{MS} scheme, provide fits at LO, NLO and NNLO (their respective sets are labeled as MSTW2008LO, MSTW2008NLO and MSTW2008NNLO).

In each case, the sets include 20 eigenvectors spanning the uncertainty of the PDFs defined at a fixed value of α_s , coming from the combinations of the 20 free parameters determined from the global analysis. The MSTW2008 PDFs consist of a central PDF set and 40 eigenvector error sets for each fit, corresponding to either a 68% or 90% CL limit. In addition, two PDF sets (at 68% and 90% CL) are available (for each of the three orders of perturbation theory considered) where the PDF fit is kept fixed while α_s is allowed to vary accordingly within the experimental errors. The fit incorporates a large amount of data from fixed-target experiments, HERA and the Tevatron (which cover a range from 0.0001 to 0.5 in x), starting from input parton distributions parameterized at $Q_0^2 = 1$ GeV. Several theoretical refinements and developments in the fitting procedure have been introduced, as treatment of heavy flavors in a general-mass variable flavor number scheme, extended input parameterization for strange quarks and gluon distributions and a new treatment of PDF uncertainties.

• HERAPDF

The HERAPDF1.0 set is based on the combination of published H1 and ZEUS measurements from HERA I on inclusive DIS in neutral (NC) and charged current (CC) reaction [16]. The PDF fit is performed at NLO using a variable-flavour-number scheme and includes error PDF sets parametrizing experimental and model uncertainties. In addition preliminary PDF sets at NNLO for two different choices of α_s [17, 18] and a NLO "dissident" variant with relaxed assumptions on light sea symmetry at low x [18] are provided.

• ABKM09

The ABKM09 PDF fit is performed at NLO and NNLO using a fixed-flavour-number scheme and is based on DIS measurements and fixed target Drell-Yan production [19]. A strong coupling constant $\alpha_s = 0.1135$ is measured at NNLO. For each of the 25 parameters of the fit a single symmetrized PDF error set is provided instead of two different sets corresponding to up- and downward variations as given by e.g. CTEQ and MSTW.

For the calculations discussed below, the values of α_s are taken from PDFs and are listed in Table II.

| PDF | CTEQ6.6/CT10/CT10W | ABKM09 | HERA1.0 | MSTW2008 | | |
|------------|--------------------|----------|---------|----------|---------|---------|
| QCD order | NLO | NLO/NNLO | NLO | LO | NLO | NNLO |
| α_s | 0.118 | 0.1135 | 0.1176 | 0.13939 | 0.12018 | 0.11707 |

TABLE II: α_s values at the scale of M_Z of different PDF sets.

D. Procedure for Determining Cross-section Uncertainties

We estimate uncertainties on cross sections from missing higher order QCD corrections, PDF and α_s uncertainties. Due to the nature of perturbative calculations, truncated fixed order calculations are usually dependent on factorization (μ_F) and renormalization (μ_R) scales. These dependences are remnants of missing higher order QCD corrections and are customarily referred to the scale dependence. We obtain the central value of a cross section by setting both μ_F and μ_R to the natural energy scale Q of a process and estimate its uncertainty by varying both scales up-and-down by a factor of two.

Uncertainties from PDF are estimated using PDF error sets. As mentioned above, CTEQ6.6 has 44 error sets, corresponding to ± 1 standard-deviation of 22 orthogonal eigen vector in the parameter space of the PDF fit. Similarly, MSTW2008 has 40 error sets of 20 orthogonal eigen vectors. For each eigen vector i , we compute cross sections σ_+^i and σ_-^i for the ± 1 standard-deviation error PDF set. The uncertainties on cross sections are then calculated using either a symmetric prescription

$$\Delta\sigma_+ = \Delta\sigma_- = \frac{1}{2} \sqrt{\sum_i (\sigma_+^i - \sigma_-^i)^2}$$

or an asymmetric prescription

$$\Delta\sigma_+ = \sqrt{\sum_i [\max(\sigma_+^i - \sigma_0, \sigma_-^i - \sigma_0, 0)]^2}, \quad \Delta\sigma_- = \sqrt{\sum_i [\max(\sigma_0 - \sigma_+^i, \sigma_0 - \sigma_-^i, 0)]^2}$$

Here σ_0 is the central value computed with the nominal PDF set. Despite of apparent differences, actually uncertainties of the two computations are found to be very similar. CTEQ PDFs include only fits at 90%CL while MSTW2008 has fits both at 68% and 90%CL.

II. $W \rightarrow \ell\nu$ AND $Z(\gamma^*) \rightarrow \ell\ell$ CROSS SECTIONS

Inclusive $W \rightarrow \ell\nu$ and $Z(\gamma^*) \rightarrow \ell\ell$ (here ℓ represents one lepton flavor) production cross sections have been calculated up to NLO using MCFM and MC@NLO and to NNLO using FEWZ and ZWPROD in QCD corrections. $Z(\gamma^*) \rightarrow \ell\ell$ cross sections are calculated for several different dilepton mass ($M_{\ell\ell}$) ranges while no mass requirement is applied to $W \rightarrow \ell\nu$ in general. ZWPROD calculates the total W and Z cross sections in the zero-width approximation and no photon exchange is included for the case of Z . In this case, $W \rightarrow \ell\nu$ and $Z \rightarrow \ell\ell$ cross sections are obtained by multiplying the total cross sections by decay branching ratios obtained using the parameter values listed in Table I. Throughout this section, $Z \rightarrow \ell\ell$ denotes pure Z contribution with γ^* -exchange switched off.

A. Results from Different Programs and PDFs

The NLO cross sections of different calculations with MSTW2008NLO and CTEQ6.6 PDF sets are compared in Table III. QCD factorization (μ_F) and renormalization (μ_R) scales are set to be the respective vector boson mass M_V ($V = W, Z$). The agreements between MCFM and FEWZ are better than 0.5% while the results from MC@NLO are generally smaller by (1–3)% than those of the other two programs. Possible sources of these small differences include hard-coded parameter values, different calculation implementations, and inconsistent parameter inputs etc. For example, while FEWZ takes partial $W \rightarrow \ell\nu$ and $Z \rightarrow \ell\ell$ decay widths as input, MCFM calculates these partial widths internally in the G_μ scheme.

| Process | $M_{\ell\ell}$ (GeV) | Scale ($\mu_F = \mu_R$) | CTEQ6.6 | | | MSTW2008NLO | | |
|---------------|-------------------------|------------------------------|--------------|--------------|--------------|--------------|--------------|-------|
| | | | MCFM | MC@NLO | FEWZ | MCFM | MC@NLO | FEWZ |
| W^+ | – | M_W | 6074(+1.7%) | 5982(+0.2%) | 6044(+1.2%) | 5975(+0.1%) | 5907(–1.1%) | 5970 |
| W^- | – | M_W | 4123(–1.5%) | 4058(–3.1%) | 4103(–2.0%) | 4206(+0.5%) | 4140(–1.1%) | 4186 |
| W^\pm | – | M_W | 10197(+0.4%) | 10040(–1.1%) | 10147(–0.1%) | 10180(+0.2%) | 10047(–1.1%) | 10155 |
| $Z(\gamma^*)$ | > 60 | M_Z | 958(–0.4%) | 953(–0.9%) | 961(–0.1%) | 956(–0.6%) | 954(–0.8%) | 962 |
| | 60 – 120 | M_Z | 948(–0.4%) | 943(–0.9%) | 951(–0.1%) | 946(–0.6%) | 944(–0.8%) | 952 |
| | 66 – 116 | M_Z | 935(–0.3%) | 929(–1.0%) | 937(–0.1%) | 933(–0.5%) | 930(–0.5%) | 938 |
| | 70 – 110 | M_Z | 923(–0.3%) | 916(–1.1%) | 925(–0.1%) | 921(–0.5%) | 917(–1.0%) | 926 |
| | 80 – 100 | M_Z | 877(–0.2%) | 870(–1.0%) | 878(–0.1%) | 875(–0.5%) | 870(–1.0%) | 879 |

TABLE III: Comparisons of NLO $W \rightarrow \ell\nu$ and $Z(\gamma^*) \rightarrow \ell\ell$ cross sections (in pb) obtained from MCFM, MC@NLO and FEWZ programs with CTEQ6.6 and MSTW2008NLO PDFs. The numbers in parentheses are relative differences to the FEWZ cross sections with the MSTW2008NLO PDF.

Table IV compares the NLO $W \rightarrow \ell\nu$ and $Z \rightarrow \ell\ell$ cross sections from a wide sample of PDFs. These cross sections are obtained from the ZWPROD program and therefore no γ^* contribution and mass requirement are included for the $Z \rightarrow \ell\ell$. While the agreements between the cross section results from MSTW and CTEQ global-fit PDFs are generally good (within 2%), the differences are large for non global-fit PDFs. Also included in the table are cross section ratios.

| Process | Scale ($\mu_F = \mu_R$) | Parton density functions | | | | | | |
|----------------------|------------------------------|--------------------------|---------------|---------------|---------------|---------------|---------------|---------------|
| | | MSTW2008 | CTEQ6.6 | CT10 | CT10W | ABKM09(5FL) | HERA1.0(NLO) | “dissident” |
| W^+ | M_W | 5996 | 6069(+1.2%) | 6017(+0.3%) | 5997(+0.0%) | 6346(+5.8%) | 6170(+2.9%) | 5468(–8.9%) |
| W^- | M_W | 4200 | 4115(–2.4%) | 4110(–2.2%) | 4151(–1.2%) | 4259(+1.4%) | 4298(+2.3%) | 4162(–0.9%) |
| W^\pm | M_W | 10197 | 10184(–0.1%) | 10127(–0.7%) | 10148(–0.5%) | 10605(+4.0%) | 10468(+2.7%) | 9629(–5.6%) |
| Z | M_Z | 946 | 946(+0.1%) | 941(–0.6%) | 943(–0.3%) | 981(+3.7%) | 969(+2.3%) | 911(–3.8%) |
| Cross section ratios | | | | | | | | |
| W^+/W^- | | 1.428 | 1.475(+3.3%) | 1.464(+2.5%) | 1.445(+1.2%) | 1.490(+4.4%) | 1.436(+0.6%) | 1.324(–8.0%) |
| W^+/W^\pm | | 0.588 | 0.596(+1.4%) | 0.594(+1.0%) | 0.591(+0.5%) | 0.598(+1.7%) | 0.589(+0.2%) | 0.568(–3.4%) |
| \mathcal{A} | | 0.176 | 0.192(+8.9%) | 0.188(+6.9%) | 0.182(+3.2%) | 0.197(+11.8%) | 0.179(+1.6%) | 0.136(–23.0%) |
| W^+/Z | | 6.336 | 6.417(+1.3%) | 6.393(+0.9%) | 6.356(+0.3%) | 6.468(+2.0%) | 6.370(+0.5%) | 6.003(–5.3%) |
| W^-/Z | | 4.438 | 4.351(–2.0%) | 4.367(–1.6%) | 4.400(–0.9%) | 4.340(–2.2%) | 4.437(–0.0%) | 4.569(+3.0%) |
| W^\pm/Z | | 10.774 | 10.768(–0.1%) | 10.760(–0.1%) | 10.756(–0.2%) | 10.808(+0.3%) | 10.807(+0.3%) | 10.572(–1.9%) |

TABLE IV: NLO $W \rightarrow \ell\nu$ and $Z \rightarrow \ell\ell$ cross sections in pb and cross section ratios calculated by ZWPROD with different PDFs. The numbers in parentheses are relative changes from the values obtained using the MSTW2008 NLO PDF. The “dissident” here refers to the PDF fits with different assumptions [20].

Cross sections with QCD corrections up to NNLO are calculated using the FEWZ and ZWPROD programs with

the MSTW2008NNLO PDF. The results are listed in Table V. Also included in the table are cross sections at LO and NLO from the same program. The cross section increases by $\sim 24\%$ from LO to NLO and by $\sim 3\%$ from NLO to NNLO. Table VI shows ratios of production cross sections, again for both calculations. The cross sections of the two calculations agree within 0.5% and the ratios agree better than 0.2%. We have therefore taken advantage of the speed of ZWPROD calculation for studying uncertainties below.

| Process | $M_{\ell\ell}$ (GeV) | Scale ($\mu_F = \mu_R$) | QCD Order | | | K-factor | |
|----------------------------|-------------------------|------------------------------|-------------|--------------|--------------|----------|----------|
| | | | LO | NLO | NNLO | NLO/LO | NNLO/NLO |
| Cross sections from FEWZ | | | | | | | |
| W^+ | — | M_W | 4936 | 5970 | 6157 | 1.21 | 1.032 |
| W^- | — | M_W | 3366 | 4186 | 4298 | 1.24 | 1.028 |
| W^\pm | — | M_W | 8301 | 10155 | 10455 | 1.22 | 1.030 |
| $Z(\gamma^*)$ | > 60 | M_Z | 778 | 962 | 989 | 1.24 | 1.029 |
| | $60 - 120$ | M_Z | 770 | 952 | 978 | 1.24 | 1.030 |
| | $66 - 116$ | M_Z | 758 | 938 | 964 | 1.24 | 1.029 |
| | $70 - 110$ | M_Z | 748 | 926 | 952 | 1.24 | 1.030 |
| | $80 - 100$ | M_Z | 710 | 879 | 904 | 1.24 | 1.029 |
| Z | — | M_Z | 766 | 943 | 969 | 1.23 | 1.028 |
| Cross sections from ZWPROD | | | | | | | |
| W^+ | — | M_W | 4930(−0.1%) | 5996(+0.4%) | 6189(+0.5%) | 1.22 | 1.032 |
| W^- | — | M_W | 3356(−0.3%) | 4200(+0.3%) | 4316(+0.4%) | 1.25 | 1.028 |
| W^\pm | — | M_W | 8286(−0.2%) | 10197(+0.4%) | 10506(+0.5%) | 1.23 | 1.030 |
| Z | — | M_Z | 764(−0.3%) | 946(+0.3%) | 974(+0.5%) | 1.24 | 1.029 |

TABLE V: $W \rightarrow \ell\nu$, $Z(\gamma^*) \rightarrow \ell\ell$ and $Z \rightarrow \ell\ell$ cross sections in pb up to LO, NLO and NNLO in QCD corrections calculated from FEWZ and ZWPROD using the MSTW2008NNLO PDF set. Note the difference between the notations $Z(\gamma^*)$ and Z , the former includes γ^* contribution while the latter does not. The numbers in parentheses of the ZWPROD cross sections are relative differences with respect to the corresponding FEWZ cross sections.

The NNLO cross sections and their ratios calculated using ZWPROD for three NNLO PDF sets are shown in Table VII. Up to 6% of the relative difference is observed for the cross sections. ABKM09 PDF predicts a particularly large charge asymmetry \mathcal{A} of W^+ and W^- productions.

B. Estimations of Uncertainties

We estimate cross section uncertainties from their dependences on factorization and renormalization scales, PDF sets and α_s values.

- Scale uncertainties: Scale uncertainties are calculated by varying the factorization and renormalization scales independently up-and-down by a factor of two around their central values with the constraint $0.5 \leq \mu_F/\mu_R \leq 2$. The maximum changes in the resulting cross sections are taken as scale uncertainties. These uncertainties are found to be $\sim \pm(2.5 - 3.5)\%$ at NLO and $\sim \pm 0.6\%$ at NNLO. Figure 1 illustrates the scale dependences of three scenarios: varying the two scales one at a time while keeping the other fixed at its central value and varying

| Cross section ratios | FEWZ | | | ZWPROD | | |
|-------------------------|--------|--------|--------|--------|--------|--------|
| | LO | NLO | NNLO | LO | NLO | NNLO |
| W^+/W^- | 1.466 | 1.426 | 1.433 | 1.469 | 1.428 | 1.434 |
| W^+/W^\pm | 0.595 | 0.588 | 0.590 | 0.695 | 0.588 | 0.589 |
| \mathcal{A} | 0.189 | 0.176 | 0.178 | 0.190 | 0.176 | 0.178 |
| W^+/Z | 6.444 | 6.331 | 6.355 | 6.453 | 6.338 | 6.355 |
| W^-/Z | 4.394 | 4.439 | 4.435 | 4.393 | 4.440 | 4.431 |
| W^\pm/Z | 10.837 | 10.769 | 10.790 | 10.846 | 10.779 | 10.786 |

TABLE VI: $W \rightarrow \ell\nu$, $Z(\gamma^*) \rightarrow \ell\ell$ and $Z \rightarrow \ell\ell$ cross section ratios (see Section IID for definitions) at LO, NLO and NNLO in QCD corrections calculated from FEWZ and ZWPROD using the MSTW2008 PDF set. Z here represents the total $Z \rightarrow \ell\ell$ cross section without γ^* contribution and mass requirement.

| Process | Scale ($\mu_F = \mu_R$) | Parton density functions | | | |
|----------------------|------------------------------|--------------------------|---------------------|---------------------|---------------------|
| | | MSTW2008NNLO | ABKM09 | HERA1.0(NNLO) | |
| | | $\alpha_s = 0.1171$ | $\alpha_s = 0.1135$ | $\alpha_s = 0.1145$ | $\alpha_s = 0.1176$ |
| W^+ | M_W | 6189 | 6416 (+3.7%) | 6423 (+3.8%) | 6544 (+5.7%) |
| W^- | M_W | 4316 | 4295 (-0.5%) | 4416 (+2.3%) | 4484 (+3.9%) |
| W^\pm | M_W | 10506 | 10711 (+2.0%) | 10839 (+3.2%) | 11028 (+5.0%) |
| Z | M_Z | 974 | 991 (+1.8%) | 1005 (+3.2%) | 1025 (+5.2%) |
| Cross section ratios | | | | | |
| W^+/W^- | | 1.434 | 1.494 (+4.2%) | 1.454 (+1.4%) | 1.459 (+1.8%) |
| W^+/W^\pm | | 0.589 | 0.599 (+1.7%) | 0.593 (+0.6%) | 0.593 (+0.7%) |
| \mathcal{A} | | 0.178 | 0.198 (+11.0%) | 0.185 (+3.8%) | 0.187 (+4.7%) |
| W^+/Z | | 6.355 | 6.473 (+1.9%) | 6.391 (+0.6%) | 6.386 (+0.5%) |
| W^-/Z | | 4.431 | 4.334 (-2.2%) | 4.394 (-0.8%) | 4.377 (-1.2%) |
| W^\pm/Z | | 10.790 | 10.81 (+0.2%) | 10.79 (+0.0%) | 10.76 (-0.2%) |

TABLE VII: NNLO $W \rightarrow \ell\nu$ and $Z \rightarrow \ell\ell$ cross sections in pb and cross section ratios calculated by ZWPROD with different PDFs. The numbers in parentheses are relative changes from the values obtained using MSTW2008 NNLO PDF.

the two scales together. The dependences on scales are significantly reduced from LO to NNLO as shown in Fig. 2 for the case of $\mu_F = \mu_R$. We have also studied cross section dependences on dynamics scales using the MCFM program. The program is modified to allow scale variations (assuming $\mu_F = \mu_R$) between $[0.5, 2] \times \sqrt{\hat{s}}$, where $\sqrt{\hat{s}}$ is the center-of-mass energy of the hard scattering process. The changes in W and $Z(\gamma^*)$ NLO cross sections are found to be $\sim \pm 1.3\%$, similar to those from variations of static scales between $[0.5, 2] \times M_V$.

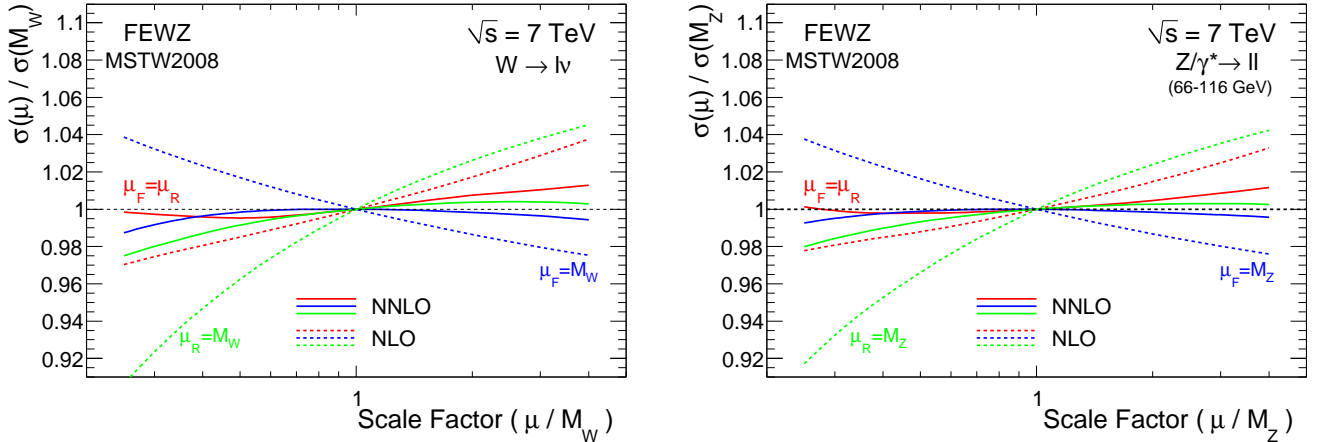


FIG. 1: Factorization and renormalization scale dependences of $W \rightarrow \ell\nu$ (left) and $Z(\gamma^*) \rightarrow \ell\ell$ (right) cross sections at NLO and NNLO. The cross sections are normalized to their values at scales $\mu_F = \mu_R = M_V$. The scales μ_F and μ_R are varied one at a time while fixing the other at M_V or are varied together. All cross sections are calculated from the FEWZ program with MSTW2008 PDF sets.

- **PDF uncertainties:** The uncertainties arising from PDFs are estimated using PDF eigenvector error sets following the procedure discussed in Section ID. The uncertainties of NLO and NNLO calculations from 68% CL error sets vary between $\sim \pm(1.6 - 2.0)\%$. They are found to be about a factor of two larger using 90%CL error sets, suggesting non-Gaussian distributions of the cross section variations. Table VIII compares the 90%CL PDF uncertainties of the NLO cross sections calculated using ZWPROD with different PDFs. The uncertainty varies between (3 – 4)%. This uncertainty is generally reduced for most of the cross section ratios.
- **α_s value and its uncertainties:** The uncertainties from α_s are estimated using MSTW2008 fits which include PDF sets with α_s values corresponding to ± 1 standard-deviation from its central value as well as values between 0.110 – 0.130. The changes in cross sections from PDF sets corresponding to 68% CL uncertainty in α_s value are about 1.1% while the 90% CL delivers around 2.6%. Using dedicated NNLO HERAPDF1.0 fits with $\alpha_s = 0.1145$ and $\alpha_s = 0.1176$ for estimating the α_s induced uncertainty, the resulting uncertainties on the cross sections are 1.9% for W^+ , 1.5% for W^- , 1.7% for W and 1.9% for Z .

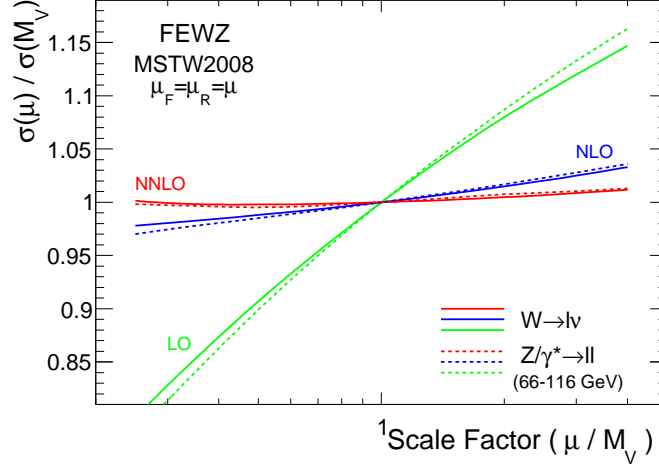


FIG. 2: Dependences of $W \rightarrow \ell\nu$ and $Z(\gamma^*) \rightarrow \ell\ell$ cross sections on QCD scales at LO, NLO and NNLO assuming $\mu_F = \mu_R$. The cross sections are normalized to their values at scales $\mu_F = \mu_R = M_V$. All cross sections are calculated from the FEWZ program with MSTW2008 PDF sets.

Figure 3 (left) shows the relative dependences on α_s of the NLO and NNLO $Z(\gamma^*) \rightarrow \ell\ell$ cross sections for $70 < M_{\ell\ell} < 110$ GeV. Similar dependences of the NLO W and $Z(\gamma^*)$ cross sections as calculated from the MCFM program are shown in Fig. 3 (right).

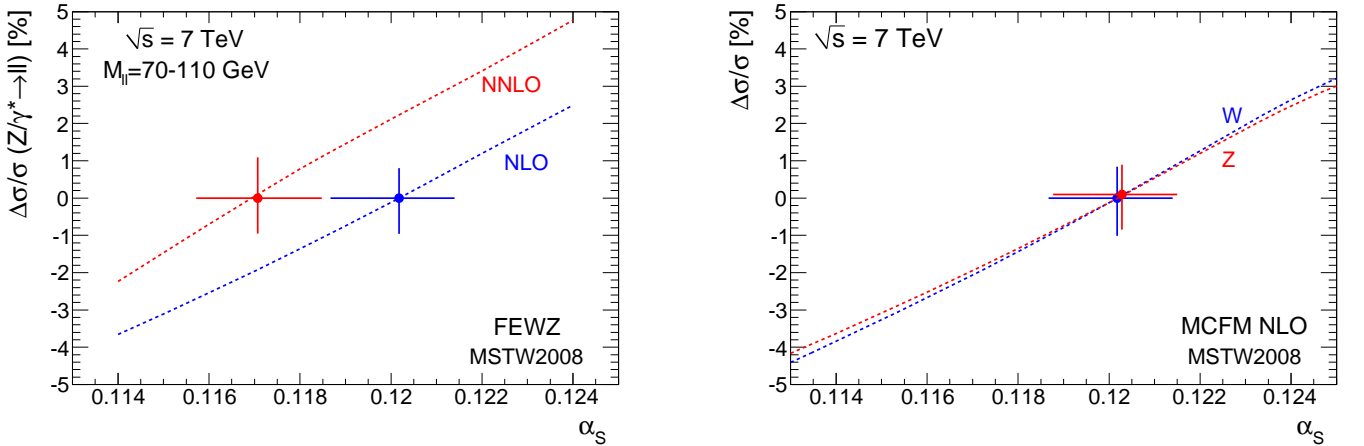


FIG. 3: Cross section changes as functions of α_s . Left: $Z(\gamma^*) \rightarrow \ell\ell$ at NLO and NNLO from the FEWZ program. Right: $W \rightarrow \ell\nu$ and $Z(\gamma^*) \rightarrow \ell\ell$ at NLO from the MCFM program. MSTW2008 PDF fits are used for all cases. The cross sections are normalized to their values at the nominal α_s values of their respective PDF sets. The horizontal bars represent the 68% CL uncertainty of α_s while the vertical bars are the ranges of resulting changes in the relative cross sections.

The combined PDF and α_s uncertainties of the NNLO cross sections and their ratios following the procedure proposed in Ref. [21] are shown in Table IX at both 68%CL and 90%CL. For the cross sections, the variation is typically around 2.5% and 4.5% at 68%CL and 90%CL respectively. The variations on the cross section ratios are generally smaller.

C. Electroweak Radiative Corrections

While QCD corrections dominate for $W \rightarrow \ell\nu$ and $Z(\gamma^*) \rightarrow \ell\ell$ processes, the electroweak radiative corrections are also important, particularly for $Z(\gamma^*) \rightarrow \ell\ell$ cross sections with invariant mass requirements. These corrections are dominated by mass-singular photonic radiations with photons generally being collinear to leptons. However, the detector acceptance estimated using Pythia Monte Carlo interfaced to PHOTOS should have corrected for most of

| Process | Parton density functions | | | |
|--|--------------------------|--------------|--------------|--------------|
| | MSTW2008 | CTEQ6.6 | CT10 | CT10W |
| Relative 90%CL PDF uncertainties of the cross sections (%) | | | | |
| W^+ | (+3.7, -3.4) | (+3.3, -3.2) | (+3.5, -4.2) | (+3.5, -4.0) |
| W^- | (+3.6, -3.6) | (+3.5, -3.7) | (+3.6, -4.1) | (+3.8, -4.1) |
| W^\pm | (+3.6, -3.3) | (+3.3, -3.3) | (+3.4, -4.0) | (+3.6, -4.0) |
| Z | (+3.6, -3.3) | (+3.2, -3.2) | (+3.3, -3.8) | (+3.5, -3.7) |
| Relative 90%CL PDF uncertainties of the cross section ratios (%) | | | | |
| W^+/W^- | (+2.1, -1.3) | (+1.6, -1.6) | (+1.8, -2.3) | (+1.4, -1.9) |
| W^+/W^\pm | (+0.9, -0.5) | (+0.6, -0.6) | (+0.7, -0.9) | (+0.6, -0.8) |
| \mathcal{A} | (+5.7, -3.6) | (+3.9, -3.9) | (+4.5, -5.8) | (+3.6, -5.0) |
| W^+/Z | (+1.0, -0.7) | (+1.0, -1.0) | (+1.4, -2.2) | (+1.2, -1.8) |
| W^-/Z | (+0.8, -1.2) | (+1.0, -1.0) | (+1.3, -1.7) | (+1.1, -1.4) |
| W^\pm/Z | (+0.3, -0.4) | (+0.6, -0.7) | (+1.0, -1.7) | (+0.9, -1.4) |

TABLE VIII: Relative 90%CL PDF uncertainties (in percent) of NLO $W \rightarrow \ell\nu$ and $Z \rightarrow \ell\ell$ cross sections calculated from ZWPROD for global-fit PDFs fits.

| Process/ Quantity | Relative uncertainty (%) | | | | |
|---------------------------------------|--------------------------|-----------------|--------------|----------------------------------|--------------|
| | Scale | PDF+ α_s | | 90%CL PDF and HERA α_s | Total |
| | | (68%CL) | (90%CL) | | |
| Uncertainties on cross sections | | | | | |
| W^+ | (+0.5, −0.8) | (+2.6, −2.0) | (+4.9, −4.1) | 3.9 | (+4.9, −4.2) |
| W^- | (+0.6, −0.8) | (+2.5, −1.9) | (+4.4, −4.2) | 3.7 | (+4.4, −4.3) |
| W^\pm | (+0.5, −0.8) | (+2.6, −2.0) | (+4.7, −4.1) | 3.7 | (+4.7, −4.2) |
| Z | (+0.5, −0.7) | (+2.5, −1.9) | (+4.5, −3.9) | 3.8 | (+4.5, −4.0) |
| Uncertainties on cross section ratios | | | | | |
| W^+/W^- | (+0.11, −0.09) | (+1.0, −0.7) | (+2.2, −1.4) | | (+2.2, −1.4) |
| W^+/W^\pm | (+0.05, −0.04) | (+0.4, −0.3) | (+0.9, −0.6) | | (+0.9, −0.6) |
| \mathcal{A} | (+0.3, −0.3) | (+2.8, −1.9) | (+6.1, −3.9) | | (+6.1, −3.9) |
| W^+/Z | (+0.04, −0.15) | (+0.5, −0.4) | (+1.2, −0.9) | | (+1.2, −0.9) |
| W^-/Z | (+0.09, −0.10) | (+0.4, −0.6) | (+0.8, −1.2) | | (+0.8, −1.2) |
| W^\pm/Z | (+0.06, −0.13) | (+0.2, −0.2) | (+0.5, −0.5) | | (+0.5, −0.5) |

TABLE IX: Summary of scale and PDF+ α_s uncertainties of W and Z cross sections and their ratios calculated to NNLO QCD using ZWPROD. The MSTW2008NNLO PDF error sets corresponding to different values of α_s and are evaluated at 68% and 90% CL, respectively, following the prescription of Ref. [21]. The second last column indicates the results obtained using averaged MSTW2008NNLO 90%CL PDF errors and the α_s uncertainties obtained from the HERAPDF1.0 NNLO fits. The last column is the quadratic sum of scale and 90%CL PDF+ α_s variations.

these radiation effects. The residual corrections are believed to be negligible. Thus our recommended cross sections below do not include any electroweak corrections.

D. Recommendations

In this note, we have adapted the approach to use the MSTW2008NNLO 90%CL PDF+ α_s uncertainties as shown in Table IX. We combine the PDF+ α_s uncertainty with that from the scale variation in quadrature to arrive at a total theoretical uncertainty. As shown in the last column of the table, the total uncertainties vary between (4–5)% for W and Z cross sections. For simplicity, we recommend to take central values from QCD NNLO calculations by FEWZ and quote a conservative 5% total theoretical uncertainty for the estimation of the expected event numbers. This uncertainty is consistent with the differences of MSTW2008, ABKM09 and HERA1.0 NNLO predictions. Table X summarizes our recommendations.

| | |
|--|--|
| $\sigma(W^+ \rightarrow \ell^+ \nu)$ | $= 6.16 \pm 0.31$ nb |
| $\sigma(W^- \rightarrow \ell^- \nu)$ | $= 4.30 \pm 0.21$ nb |
| $\sigma(W^\pm \rightarrow \ell^\pm \nu)$ | $= 10.46 \pm 0.52$ nb |
| $\sigma(Z(\gamma^*) \rightarrow \ell\ell)$ | $= 0.964 \pm 0.048$ nb ($66 < M_{\ell\ell} < 116$ GeV) |
| $\sigma(Z(\gamma^*) \rightarrow \ell\ell)$ | $= 1.070 \pm 0.054$ nb ($40 < M_{\ell\ell} < 2000$ GeV) |
| $\sigma(Z(\gamma^*) \rightarrow \ell\ell)$ | $= 0.989 \pm 0.049$ nb ($M_{\ell\ell} > 60$ GeV) |
| $\sigma(Z \rightarrow \ell\ell)$ | $= 0.969 \pm 0.048$ nb |
| $\sigma(Z \rightarrow \ell\ell)$ | $= 0.944 \pm 0.047$ nb ($66 < M_{\ell\ell} < 116$ GeV) |

TABLE X: Summary of $W \rightarrow \ell\nu$ and $Z(\gamma^*) \rightarrow \ell\ell$ (ℓ = one lepton flavor) cross sections calculated to NNLO QCD and associated total systematic uncertainties of 5%. Note that the $Z \rightarrow \ell\ell$ cross sections above do not include γ^* contributions.

Ratios of cross sections allow for cancelations of many uncertainties and therefore are often measured with better precisions than the cross sections themselves. For their theoretical predictions, we once again recommend to take the central values from the NNLO FEWZ calculations. The QCD scale dependence of the cross sections generally cancels in the ratio. Consequently, the scale uncertainty is negligible ($\sim 0.1 - 0.3\%$). The PDF+ α_s 90%CL uncertainty is found to be $\sim (1 - 2)\%$ for most of the ratios, but is as large as 6% for \mathcal{A} as shown in Table IX. Our recommendations for the cross section ratios are summarized in Table XI.

| | | |
|---|--|-----------------------------|
| $\frac{\sigma(W^+ \rightarrow \ell^+ \nu)}{\sigma(W^- \rightarrow \ell^- \nu)}$ | $= 1.433 \times (1.000^{+0.022}_{-0.014})$ | $= 1.433^{+0.032}_{-0.020}$ |
| $\frac{\sigma(W^+ \rightarrow \ell^+ \nu)}{\sigma(W^\pm \rightarrow \ell^\pm \nu)}$ | $= 0.590 \pm (1.000^{+0.009}_{-0.006})$ | $= 0.590^{+0.005}_{-0.004}$ |
| $\mathcal{A} = \frac{\sigma(W^+ \rightarrow \ell^+ \nu) - \sigma(W^- \rightarrow \ell^- \nu)}{\sigma(W^+ \rightarrow \ell^+ \nu) + \sigma(W^- \rightarrow \ell^- \nu)}$ | $= 0.178 \times (1.000^{+0.061}_{-0.039})$ | $= 0.178^{+0.011}_{-0.007}$ |
| $\frac{\sigma(W^+ \rightarrow \ell^+ \nu)}{\sigma(Z \rightarrow \ell\ell)}$ | $= 6.355 \times (1.000^{+0.012}_{-0.009})$ | $= 6.355^{+0.076}_{-0.057}$ |
| $\frac{\sigma(W^- \rightarrow \ell^- \nu)}{\sigma(Z \rightarrow \ell\ell)}$ | $= 4.435 \times (1.000^{+0.008}_{-0.012})$ | $= 4.435^{+0.035}_{-0.053}$ |
| $\frac{\sigma(W^\pm \rightarrow \ell^\pm \nu)}{\sigma(Z \rightarrow \ell\ell)}$ | $= 10.790 \times (1.000 \pm 0.005)$ | $= 10.790 \pm 0.054$ |

TABLE XI: Summary of cross section ratios and their estimated theoretical uncertainties. Note that W/Z cross section ratios above are normalized to $Z \rightarrow \ell\ell$ cross section without the γ^* contribution and the requirement on the dilepton mass.

The W/Z cross section ratios normalized to $Z(\gamma^*) \rightarrow \ell\ell$ cross section in the mass window $66 < M_{\ell\ell} < 116$ GeV are

| | | |
|---|--|-----------------------------|
| $\frac{\sigma(W^+ \rightarrow \ell^+ \nu)}{\sigma(Z(\gamma^*) \rightarrow \ell\ell)}$ | $= 6.387 \times (1.000^{+0.012}_{-0.009})$ | $= 6.387^{+0.077}_{-0.057}$ |
| $\frac{\sigma(W^- \rightarrow \ell^- \nu)}{\sigma(Z(\gamma^*) \rightarrow \ell\ell)}$ | $= 4.445 \times (1.000^{+0.008}_{-0.012})$ | $= 4.445^{+0.036}_{-0.054}$ |
| $\frac{\sigma(W^\pm \rightarrow \ell^\pm \nu)}{\sigma(Z(\gamma^*) \rightarrow \ell\ell)}$ | $= 10.840 \times (1.000 \pm 0.005)$ | $= 10.840 \pm 0.054$ |

We caution that these ratios may show different kinematic dependencies which have to be evaluated carefully for the chosen binning and phase space cuts. Moreover, the uncertainties quoted here do not cover deviations seen using other PDF sets for some ratios, see Table VII.

E. Cross Sections for Different \sqrt{s} Values

To facilitate comparisons with cross section measurements by other experiments at different colliders, we have also calculated QCD NNLO W and Z cross sections at different values of \sqrt{s} for both pp and $p\bar{p}$ colliders. These cross sections are tabulated in Table XII and their dependences on \sqrt{s} are illustrated in Fig. 4.

| \sqrt{s} (TeV) | $p\bar{p}$ collider | | | pp collider | | | | | | |
|---------------------|---------------------|---------------|------|---------------|-------|---------|---------------|------|-------|-----------|
| | W^\pm | $Z(\gamma^*)$ | Z | W^+ | W^- | W^\pm | $Z(\gamma^*)$ | Z | A | W^\pm/Z |
| 0.4 | 332 | 30.3 | 31.4 | 68.6 | 21.7 | 90.3 | 4.4 | 4.4 | 0.519 | 20.351 |
| 0.6 | 687 | 64.6 | 65.6 | 211 | 78.3 | 289 | 19.2 | 19.2 | 0.458 | 15.061 |
| 0.63 | 736 | 69.8 | 70.4 | 234 | 89.7 | 324 | 21.3 | 22.3 | 0.446 | 14.536 |
| 0.8 | 1012 | 95.4 | 96.2 | 375 | 159 | 534 | 38.9 | 38.9 | 0.405 | 13.731 |
| 1.0 | 1321 | 124 | 124 | 549 | 254 | 803 | 61.5 | 62.5 | 0.367 | 12.845 |
| 1.2 | 1619 | 151 | 152 | 727 | 359 | 1086 | 87.0 | 88.0 | 0.339 | 12.344 |
| 1.4 | 1915 | 178 | 179 | 908 | 471 | 1379 | 113 | 113 | 0.317 | 12.169 |
| 1.6 | 2211 | 204 | 205 | 1092 | 588 | 1679 | 140 | 141 | 0.301 | 11.942 |
| 1.8 | 2508 | 231 | 233 | 1278 | 708 | 1986 | 168 | 169 | 0.287 | 11.764 |
| 1.96 | 2748 | 253 | 254 | 1427 | 808 | 2235 | 190 | 192 | 0.277 | 11.642 |
| 2.0 | 2808 | 258 | 259 | 1464 | 833 | 2296 | 196 | 197 | 0.275 | 11.654 |
| 3.0 | 4342 | 399 | 401 | 2407 | 1486 | 3893 | 343 | 345 | 0.237 | 11.282 |
| 4.0 | 5921 | 545 | 548 | 3353 | 2171 | 5524 | 495 | 498 | 0.214 | 11.103 |
| 5.0 | 7518 | 695 | 699 | 4295 | 2871 | 7166 | 651 | 654 | 0.199 | 10.953 |
| 6.0 | 9130 | 848 | 852 | 5232 | 3583 | 8815 | 807 | 811 | 0.187 | 10.872 |
| 7.0 | 10744 | 1002 | 1007 | 6157 | 4298 | 10455 | 964 | 969 | 0.178 | 10.790 |
| 8.0 | 12354 | 1157 | 1163 | 7072 | 5015 | 12087 | 1122 | 1128 | 0.170 | 10.716 |
| 9.0 | 13957 | 1312 | 1319 | 7977 | 5731 | 13708 | 1280 | 1286 | 0.164 | 10.662 |
| 10.0 | 15554 | 1467 | 1481 | 8877 | 6445 | 15322 | 1437 | 1445 | 0.159 | 10.608 |
| 11.0 | 17136 | 1623 | 1627 | 9760 | 7164 | 16924 | 1593 | 1601 | 0.153 | 10.572 |
| 12.0 | 18726 | 1777 | 1784 | 10635 | 7872 | 18507 | 1750 | 1758 | 0.149 | 10.526 |
| 13.0 | 20297 | 1932 | 1941 | 11501 | 8579 | 20080 | 1906 | 1914 | 0.145 | 10.525 |
| 14.0 | 21819 | 2086 | 2093 | 12371 | 9289 | 21659 | 2061 | 2081 | 0.142 | 10.491 |
| 15.0 | 23505 | 2239 | 2233 | 13217 | 9992 | 23209 | 2216 | 2219 | 0.139 | 10.494 |

TABLE XII: $W \rightarrow \ell\nu$ and $Z(\gamma^*) \rightarrow \ell\ell$ cross sections in pb calculated up to QCD NNLO for different center-of-mass energies of both pp and $p\bar{p}$ collisions. They are obtained from the FEWZ program using MSTW2008NNLO PDF set. $Z(\gamma^*) \rightarrow \ell\ell$ cross sections are for $66 < M_{\ell\ell} < 116$ GeV. Also shown are $Z \rightarrow \ell\ell$ cross sections with γ^* contributions turned off and no requirement on the dilepton mass.

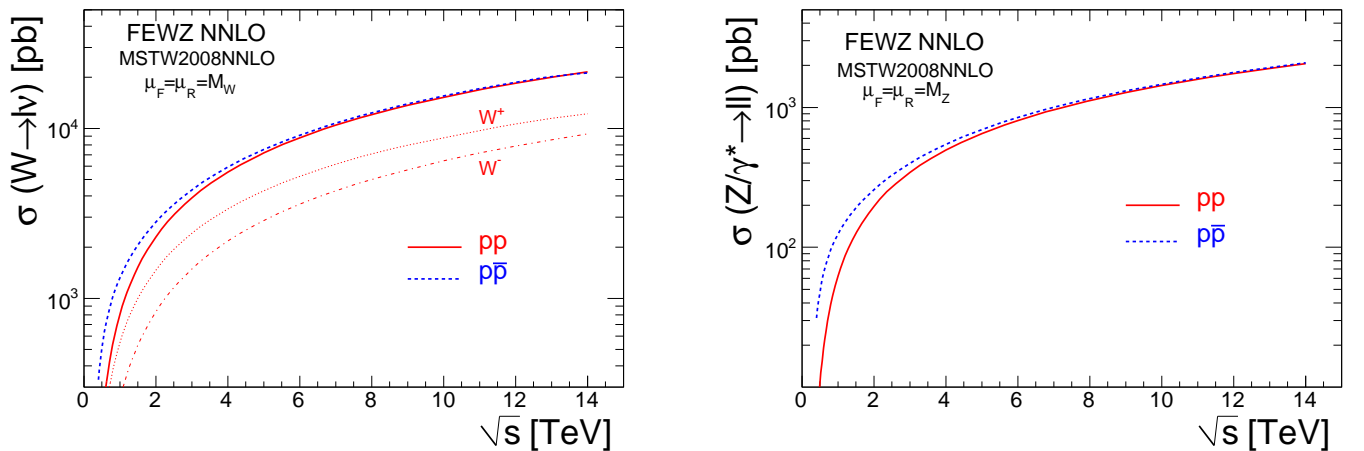


FIG. 4: The QCD NNLO $W \rightarrow \ell\nu$ (left) and $Z(\gamma^*) \rightarrow \ell\ell$ (right) cross sections as functions of \sqrt{s} for both pp and $p\bar{p}$ collisions.

III. DIBOSON PRODUCTION

A. Cross section calculations

The production of a pair of vector bosons (VV with $V = W, Z$) is dominated by $q\bar{q}'$ initiated processes ($q\bar{q}' \rightarrow VV$). These processes with up to NLO in QCD corrections have been implemented in MCFM and MC@NLO programs. Unless specified otherwise, Z includes both vector boson Z and virtual photon (γ^*) contributions in the following discussion. The treatment of the vector bosons in MCFM and MC@NLO differs. In MCFM the possibility exists, as for single bosons, to choose between on-shell or off-shell W and Z , by properly setting the option `.zerowidth..` In MC@NLO, the possibility to include also off-shell effect is implemented only for WW process when the spin correlations are on (`ILCODE=1,2,3`). For ZZ and WZ production processes, the vector bosons are always on-shell [28]. In the case of neutral vector boson, the γ -interferences are always off. For MCFM, the total inclusive VV cross sections are obtained by removing branching ratios of VV cross sections with V decaying to leptons. Branching ratios of $BR(W \rightarrow \ell\nu) = 0.1088$ and $BR(Z \rightarrow \ell\ell) = 0.0336$ are assumed regardless the mass requirement of the Z/γ^* bosons.

Table XIII compares the NLO diboson cross sections in pp collisions at $\sqrt{s} = 7$ TeV from the two calculations with different PDFs. The results are presented for different cuts on the $Z(\gamma^*)$ boson mass, namely $M_Z > 12$ GeV (the internal default cut applied in PYTHIA on Z boson mass), $M_Z > 60$ GeV and $66 < M_Z < 116$ GeV (chosen in agreement with the Z cross section analysis). The factorization and renormalization scales are set to be equal and are generally chosen to be the average mass of the vector bosons. For the ZZ process, cross sections for dynamic scales are also computed. In this case, the scale is set to be equal to the mass of the final-state ZZ system. WZ and ZZ cross sections for a few other choices of Z mass window are shown in Table XIV. The central values of the cross sections estimated with MSTW2008NLO PDF set are generally $\sim 4\%$ higher than those obtained from the CTEQ6.6 PDF set, while CT10 numbers are generally in between these two estimations. The difference is particularly large, up to $\sim 6\%$, for the W^-Z cross section between CTEQ6.6 and MSTW2008NLO. It should be noted though CT10 is the new incarnation of CTEQ6.6. The differences between CT10 and MSTW2008NLO are generally smaller than $\sim 2\%$ with the exception of the W^-Z process for which the difference is around $\sim 4\%$. HERA1.0 results are a few percent higher than those of MSTW2008 while NNPDF results are a few percent lower.

| Process | Scale ($\mu_F = \mu_R$) | M_Z (GeV) | MCFM | | | | | MC@NLO | |
|-----------|------------------------------|----------------|---------------|---------------|---------------|---------------|----------|---------------|----------|
| | | | CTEQ6.6 | CT10 | HERA1.0 | NNPDF | MSTW2008 | CTEQ6.6 | MSTW2008 |
| WW | M_W | — | 43.39 (−3.4%) | 44.00 (−2.0%) | 46.47 (+3.5%) | 43.76 (−2.6%) | 44.92 | 43.15 (−3.6%) | 44.76 |
| W^+Z | $(M_W + M_Z)/2$ | 66 – 116 | 11.28 (−1.9%) | 11.38 (−1.0%) | 11.63 (+1.1%) | 11.41 (−0.8%) | 11.50 | 11.17 (−2.3%) | 11.43 |
| W^-Z | $(M_W + M_Z)/2$ | 66 – 116 | 6.09 (−5.9%) | 6.21 (−4.0%) | 6.75 (+4.3%) | 6.26 (−3.2%) | 6.47 | 6.03 (−5.8%) | 6.40 |
| $W^\pm Z$ | $(M_W + M_Z)/2$ | 66 – 116 | 17.37 (−3.3%) | 17.59 (−2.1%) | 18.38 (+2.3%) | 17.67 (−1.7%) | 17.97 | 17.20 (−3.5%) | 17.83 |
| ZZ | M_Z | 66 – 116 | 5.47 (−3.0%) | 5.53 (−2.0%) | 5.79 (+2.7%) | 5.48 (−2.8%) | 5.64 | 5.67 (−3.5%) | 5.86 |
| | M_Z | > 60 | 5.77 (−3.2%) | 5.84 (−2.0%) | 6.12 (+2.7%) | 5.79 (−2.9%) | 5.96 | — | — |
| | M_Z | > 12 | 8.98 (−2.7%) | 9.07 (−1.7%) | 9.56 (+3.6%) | 8.98 (−2.7%) | 9.23 | — | — |
| | dynamic | 66 – 116 | 5.32 (−2.7%) | 5.37 (−1.8%) | 5.63 (+2.9%) | 5.34 (−2.4%) | 5.47 | — | — |
| | dynamic | > 60 | 5.61 (−2.8%) | 5.67 (−1.7%) | 5.95 (+3.1%) | 5.64 (−2.3%) | 5.77 | — | — |
| | dynamic | > 12 | 8.80 (−2.5%) | 8.88 (−1.7%) | 9.37 (+3.8%) | 8.81 (−2.4%) | 9.03 | — | — |
| | dynamic | > 12 | 8.80 (−2.5%) | 8.88 (−1.7%) | 9.37 (+3.8%) | 8.81 (−2.4%) | 9.03 | — | — |

TABLE XIII: Total NLO diboson cross sections in pb of pp collisions at $\sqrt{s} = 7$ TeV calculated from MCFM and MC@NLO programs for CTEQ6.6, CT10, HERA1.0, NNPDF and MSTW2008NLO PDFs. As explained in the text, in MC@NLO Z and W in diboson productions are always treated on-mass-shell, therefore the cross section is insensitive to mass cuts. The dynamic scale for ZZ is set to be the mass of the final-state ZZ system. The numbers in parentheses are relative changes from cross section values using MSTW2008NLO PDF.

B. K-Factors

Table XV compares diboson cross sections at LO and NLO in QCD corrections, calculated from the MCFM program with MSTW2008 PDF sets. The cross section increases dramatically from LO to NLO and is the largest for WZ at $\sim 72\%$.

Tables XVI and XVII show the LO and NLO WW and ZZ cross sections, together with the resulting K-factor ($= \sigma_{NLO}/\sigma_{LO}$) as a function of the mass of the four lepton final states. As appears from Fig. 5, which display graphically the results, the K-factors are quite stable, over all the mass range, with the exception of the lowest part of the spectrum, where anyway the cross sections are small and larger affected by the integration errors.

| Process | Scale ($\mu_F = \mu_R$) | $Z(\gamma^*)$ mass range in GeV | | | | | |
|-------------|------------------------------|---------------------------------|---------------|---------------|---------------|---------------|---------------|
| | | > 12 | > 60 | $60 - 120$ | $66 - 116$ | $70 - 110$ | $80 - 100$ |
| CTEQ6.6 | | | | | | | |
| W^+Z | $(M_W + M_Z)/2$ | 16.97 (−1.1%) | 11.63 (−2.0%) | 11.37 (−2.0%) | 11.28 (−1.9%) | 11.16 (−1.8%) | 10.64 (−1.9%) |
| W^-Z | $(M_W + M_Z)/2$ | 9.71 (−4.8%) | 6.27 (−5.9%) | 6.15 (−5.8%) | 6.09 (−5.9%) | 6.02 (−5.9%) | 5.74 (−5.9%) |
| $W^\pm Z$ | $(M_W + M_Z)/2$ | 26.67 (−2.6%) | 17.91 (−3.3%) | 17.52 (−3.4%) | 17.37 (−3.3%) | 17.18 (−3.4%) | 16.38 (−3.4%) |
| ZZ | M_Z | 8.98 (−2.7%) | 5.77 (−3.2%) | 5.56 (−3.0%) | 5.47 (−3.0%) | 5.36 (−2.9%) | 4.88 (−3.0%) |
| CT10 | | | | | | | |
| W^+Z | $(M_W + M_Z)/2$ | 17.06 (−0.6%) | 11.74 (−1.1%) | 11.48 (−1.0%) | 11.38 (−1.0%) | 11.26 (−1.0%) | 10.73 (−1.1%) |
| W^-Z | $(M_W + M_Z)/2$ | 9.85 (−3.4%) | 6.40 (−3.9%) | 6.26 (−4.1%) | 6.21 (−4.0%) | 6.14 (−4.1%) | 5.86 (−3.9%) |
| $W^\pm Z$ | $(M_W + M_Z)/2$ | 26.91 (−1.7%) | 18.14 (−2.1%) | 17.74 (−2.2%) | 17.59 (−2.1%) | 17.40 (−2.1%) | 16.59 (−2.1%) |
| ZZ | M_Z | 9.07 (−1.7%) | 5.84 (−2.0%) | 5.62 (−1.9%) | 5.53 (−2.0%) | 5.42 (−1.8%) | 4.94 (−1.8%) |
| MSTW2008NLO | | | | | | | |
| W^+Z | $(M_W + M_Z)/2$ | 17.16 | 11.87 | 11.60 | 11.50 | 11.37 | 10.85 |
| W^-Z | $(M_W + M_Z)/2$ | 10.20 | 6.66 | 6.53 | 6.47 | 6.40 | 6.10 |
| $W^\pm Z$ | $(M_W + M_Z)/2$ | 27.37 | 18.53 | 18.13 | 17.97 | 17.78 | 16.95 |
| ZZ | M_Z | 9.23 | 5.96 | 5.73 | 5.64 | 5.52 | 5.03 |

TABLE XIV: Total NLO $W^\pm Z$ and ZZ cross sections in pb calculated from MCFM with CTEQ6.6, CT10 and MSTW2008NLO PDFs for different $Z(\gamma^*)$ mass range. The numbers in parentheses are relative changes from the cross section values using MSTW2008NLO PDF.

| Process | Scale ($\mu_F = \mu_R$) | M_Z (GeV) | QCD order | | K-factor (NLO/LO) |
|-----------|------------------------------|----------------|-----------|-------|----------------------|
| | | | LO | NLO | |
| WW | M_W | — | 28.94 | 44.92 | 1.55 |
| W^+Z | $(M_W + M_Z)/2$ | 66 – 116 | 6.70 | 11.50 | 1.72 |
| W^-Z | $(M_W + M_Z)/2$ | 66 – 116 | 3.65 | 6.47 | 1.77 |
| $W^\pm Z$ | $(M_W + M_Z)/2$ | 66 – 116 | 10.35 | 17.97 | 1.74 |
| ZZ | M_Z | 66 – 116 | 3.97 | 5.64 | 1.42 |
| | M_Z | > 60 | 4.20 | 5.96 | 1.42 |
| | M_Z | > 12 | 6.73 | 9.23 | 1.37 |

TABLE XV: LO and NLO diboson cross sections in pb and K-factors calculated from MCFM using MSTW2008 PDF sets.

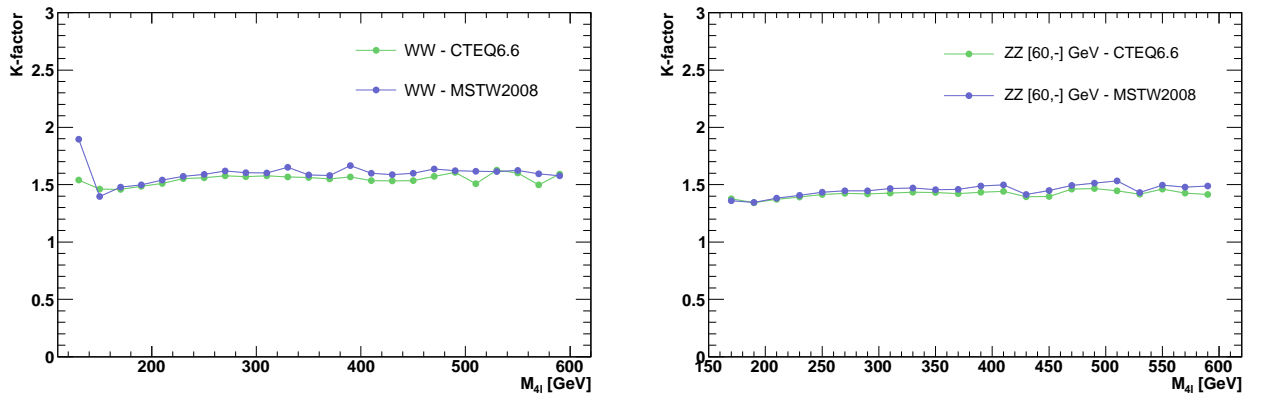


FIG. 5: Differential K-factors ($= \sigma_{NLO}/\sigma_{LO}$) vs M_{VV} for WW (left) and ZZ (right) processes. Cross sections are calculated from the MCFM program.

| $M_{4\ell}$ (GeV) | CTEQ6L1/CTEQ6.6 | | | MSTW2008LO/NLO | | |
|----------------------|-----------------|-------|----------|----------------|-------|----------|
| | LO | NLO | K-factor | LO | NLO | K-factor |
| 130 | 3.118 | 4.803 | 1.540 | 2.776 | 5.268 | 1.897 |
| 150 | 15.71 | 22.96 | 1.461 | 16.30 | 22.77 | 1.396 |
| 170 | 212.6 | 310.1 | 1.458 | 215.4 | 318.3 | 1.477 |
| 190 | 247.9 | 368.5 | 1.486 | 251.9 | 377.8 | 1.499 |
| 210 | 197.5 | 298.5 | 1.511 | 199.5 | 307.3 | 1.540 |
| 230 | 149.7 | 232.4 | 1.552 | 152.3 | 239.7 | 1.573 |
| 250 | 115.4 | 180.0 | 1.559 | 117.0 | 186.0 | 1.589 |
| 270 | 88.31 | 139.3 | 1.577 | 89.11 | 144.3 | 1.619 |
| 290 | 69.80 | 109.6 | 1.570 | 70.79 | 113.7 | 1.605 |
| 310 | 55.21 | 87.14 | 1.578 | 56.43 | 90.43 | 1.602 |
| 330 | 43.84 | 68.71 | 1.567 | 44.26 | 73.10 | 1.651 |
| 350 | 35.61 | 55.69 | 1.563 | 36.30 | 57.54 | 1.585 |
| 370 | 29.41 | 45.58 | 1.549 | 29.73 | 46.99 | 1.580 |
| 390 | 23.55 | 36.91 | 1.567 | 23.85 | 39.77 | 1.667 |
| 410 | 19.77 | 30.38 | 1.536 | 19.86 | 31.76 | 1.599 |
| 430 | 16.66 | 25.53 | 1.532 | 16.98 | 26.95 | 1.586 |
| 450 | 13.94 | 21.41 | 1.534 | 14.17 | 22.66 | 1.598 |
| 470 | 11.53 | 18.13 | 1.572 | 11.73 | 19.20 | 1.636 |
| 490 | 9.609 | 15.44 | 1.607 | 10.09 | 16.37 | 1.621 |
| 510 | 8.497 | 12.81 | 1.508 | 8.556 | 13.83 | 1.616 |
| 530 | 7.057 | 11.48 | 1.626 | 7.347 | 11.86 | 1.615 |
| 550 | 5.720 | 9.167 | 1.602 | 6.202 | 10.07 | 1.624 |
| 570 | 5.287 | 7.931 | 1.499 | 5.390 | 8.593 | 1.594 |
| 590 | 4.380 | 6.975 | 1.592 | 4.730 | 7.465 | 1.578 |

TABLE XVI: LO and NLO WW cross sections in pb and the corresponding K-factor as a function of the 4-lepton-mass bins, for two different PDF sets. Cross sections are calculated from the MCFM program.

| $M_{4\ell}$ (GeV) | CTEQ6L1/CTEQ6.6 | | | MSTW2008LO/NLO | | |
|----------------------|-----------------|-------|----------|----------------|-------|----------|
| | LO | NLO | K-factor | LO | NLO | K-factor |
| 170 | 2.327 | 3.204 | 1.376 | 2.404 | 3.274 | 1.361 |
| 190 | 31.04 | 41.71 | 1.343 | 31.56 | 42.48 | 1.345 |
| 210 | 37.63 | 51.64 | 1.372 | 38.12 | 52.74 | 1.383 |
| 230 | 29.14 | 40.57 | 1.392 | 29.58 | 41.60 | 1.406 |
| 250 | 21.87 | 30.93 | 1.414 | 22.18 | 31.80 | 1.433 |
| 270 | 16.42 | 23.40 | 1.424 | 16.69 | 24.13 | 1.445 |
| 290 | 12.65 | 17.97 | 1.420 | 12.85 | 18.60 | 1.446 |
| 310 | 9.885 | 14.12 | 1.428 | 10.00 | 14.65 | 1.465 |
| 330 | 7.756 | 11.12 | 1.434 | 7.877 | 11.59 | 1.471 |
| 350 | 6.118 | 8.760 | 1.431 | 6.241 | 9.091 | 1.456 |
| 370 | 4.980 | 7.082 | 1.422 | 5.061 | 7.387 | 1.459 |
| 390 | 4.070 | 5.843 | 1.435 | 4.108 | 6.120 | 1.489 |
| 410 | 3.303 | 4.766 | 1.442 | 3.369 | 5.050 | 1.498 |
| 430 | 2.812 | 3.920 | 1.393 | 2.862 | 4.048 | 1.414 |
| 450 | 2.328 | 3.252 | 1.396 | 2.389 | 3.459 | 1.448 |
| 470 | 1.934 | 2.829 | 1.462 | 1.986 | 2.966 | 1.493 |
| 490 | 1.640 | 2.404 | 1.466 | 1.667 | 2.525 | 1.514 |
| 510 | 1.338 | 1.935 | 1.446 | 1.359 | 2.085 | 1.534 |
| 530 | 1.192 | 1.688 | 1.416 | 1.236 | 1.770 | 1.431 |
| 550 | 0.987 | 1.443 | 1.461 | 1.007 | 1.507 | 1.497 |
| 570 | 0.845 | 1.207 | 1.427 | 0.8589 | 1.270 | 1.478 |
| 590 | 0.726 | 1.028 | 1.415 | 0.7569 | 1.127 | 1.489 |

TABLE XVII: LO and NLO ZZ cross sections in pb and the corresponding K-factor as a function of the 4-lepton-mass bins, for two different PDF sets. The Z boson mass is taken to be $M_Z > 60$ GeV. Cross sections are calculated from the MCFM program.

C. Uncertainties

Diboson cross section uncertainties from their dependences on scales, PDF and $\alpha_s(M_Z)$ values are estimated in the same way as those of the W and Z cross sections. The relative cross section changes for the selected ranges of M_Z are summarized in Table XVIII. The scale uncertainties are estimated by varying μ_F and μ_R independently up-and-down by a factor of two around their nominal value but with the constraint $0.5 \leq \mu_F/\mu_R \leq 2$. However, we note that removing this constraint only increases the scale dependence slightly. The uncertainty is found to be the largest for WZ and the smallest for ZZ . The combined PDF+ α_s uncertainties are estimated following the procedure of Ref. [21]. The dependences on α_s are also illustrated in Fig. 6 for WW and ZZ production. The uncertainties for the other $M_{Z(\gamma^*)}$ mass range studied are very similar.

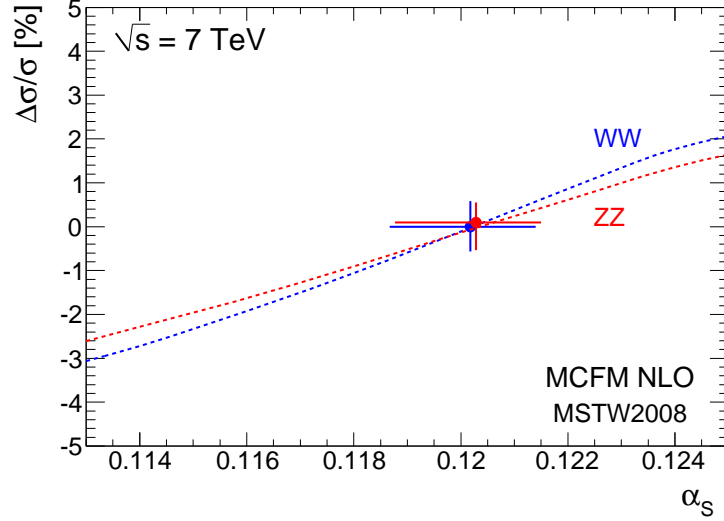


FIG. 6: Changes in NLO cross sections normalized to their nominal values as functions of α_s for WW and ZZ productions. Cross sections are calculated from the MCFM program.

| Process | $M_{Z(\gamma^*)}$ range (GeV) | Relative uncertainty (%) | | |
|-----------|----------------------------------|--------------------------|-----------------------|--------------|
| | | Scale | 90%CL PDF+ α_s | Total |
| WW | — | (+3.6, -2.9) | (+4.2, -3.5) | (+5.5, -4.5) |
| W^+Z | 66 – 116 | (+5.5, -4.2) | (+4.3, -3.4) | (+7.0, -5.5) |
| W^-Z | 66 – 116 | (+5.7, -4.3) | (+4.3, -4.0) | (+7.1, -5.9) |
| $W^\pm Z$ | 66 – 116 | (+5.5, -4.2) | (+4.3, -3.6) | (+7.0, -5.5) |
| ZZ | 66 – 116 | (+2.6, -2.1) | (+4.3, -3.5) | (+5.0, -4.1) |
| | > 60 | (+2.6, -2.1) | (+4.2, -3.6) | (+4.9, -4.2) |
| | > 12 | (+2.6, -1.9) | (+4.2, -3.3) | (+4.9, -3.8) |

TABLE XVIII: Estimated uncertainties of diboson production cross sections computed with the MCFM program with the MSTW2008NLO PDF set. The scale uncertainties from CTEQ6.6 are included in parentheses for comparisons. The total uncertainties are quadratic sum of scale and PDF+ α_s uncertainties.

D. Cross sections of $gg \rightarrow WW$ and $gg \rightarrow ZZ$

Gluon-gluon initiated processes via quark-box diagrams ($gg \rightarrow WW$ and $gg \rightarrow ZZ$) are NNLO subprocesses of WW and ZZ productions in hadron collisions. Despite of being at $\mathcal{O}(\alpha_s^2)$ relative to the $q\bar{q}'$ initiated diagrams at LO, the importance of these processes are enhanced by the large gluon flux at the LHC. The $gg \rightarrow ZZ$ process was first analyzed in Refs. [22, 23], with leptonic decays subsequently studied for on-shell [24] and off-shell [25] weak bosons. The first complete calculation of the gluon-induced loop process $gg \rightarrow Z^*(\gamma^*)Z^*(\gamma^*) \rightarrow \ell\bar{\ell}\ell'\bar{\ell}'$, allowing for arbitrary invariant masses of the Z bosons and including also the photon contributions, was presented in Ref. [10].

Neither MCFM nor MC@NLO include these processes, therefore their contributions are evaluated separately using dedicated programs **gg2WW** [9] and **gg2ZZ** [10]. Table XIX reports $gg \rightarrow WW \rightarrow e\nu e\nu$ and $gg \rightarrow ZZ \rightarrow ee\mu\mu$ cross sections, evaluated by setting the factorization and renormalization scales to their respective vector boson mass. These calculations are done by using the full matrix element, from the gg initial state to the leptons of the final state. Relative to NLO WW and ZZ cross sections discussed above, $gg \rightarrow WW$ contributes $\sim 2.9\%$ and the $gg \rightarrow ZZ$ contributes $\sim 5.7\%$ assuming $BR(W \rightarrow \ell\nu) = 0.1088$ and $BR(Z \rightarrow \ell\ell) = 0.0336$.

A detailed study of the theoretical uncertainties due to variations of the renormalization and factorization scales was performed in Ref. [27]. This study yielded a conservative error of $(^{+60}_{-35})\%$. The error due to the parton density uncertainties is less than 10%. They represent a first estimation of gluon initiated contribution to the diboson cross section, and need to be tuned before including them in the computation of the total inclusive cross sections.

| Process | M_Z (GeV) | PDFs | |
|---|----------------|---------|----------|
| | | CTEQ6.6 | MSTW2008 |
| $gg \rightarrow WW \rightarrow e\nu e\nu$ | — | 14.5 | 15.5 |
| $gg \rightarrow ZZ \rightarrow ee\mu\mu$ | > 12 | 1.14 | 1.2 |

TABLE XIX: $gg \rightarrow WW \rightarrow e\nu e\nu$ and $gg \rightarrow ZZ \rightarrow ee\mu\mu$ cross sections in fb, calculated from **gg2WW** and **gg2ZZ** programs with CTEQ6.6 and MSTW2008NLO PDFs.

E. Reference cross sections

NLO diboson cross sections are observed to vary up to $\sim 4\%$ between programs MCFM and MC@NLO and PDFs CT10 and MSTW2008NLO. Similar to the recommendations of single boson production cross sections, we suggest to quote NLO calculations from MCFM with MSTW2008NLO PDF as the reference cross sections and take combined scale and 90%CL PDF+ α_s uncertainties as the total theoretical uncertainties. As shown in the last column of Table XVIII, the total uncertainty is strongly dependent on the process. For simplicity, we suggest to assign a total theoretical uncertainty of 5% for WW and ZZ and 7% for WZ . These uncertainties are sufficient to cover the spreads observed among different calculations and PDFs. Table XX summarizes the reference total inclusive cross sections. To get cross sections for leptonic final states, W and Z branching ratios of $BR(W \rightarrow \ell\nu) = 0.1088$ and $BR(Z \rightarrow \ell\ell) = 0.0336$ should be used, regardless the Z mass requirement.

| | |
|-------------------|--|
| $\sigma(WW)$ | $= 44.9 \pm 2.2$ pb |
| $\sigma(W^+Z)$ | $= 11.5 \pm 0.8$ pb ($66 < M_Z < 116$ GeV) |
| $\sigma(W^-Z)$ | $= 6.47 \pm 0.45$ pb ($66 < M_Z < 116$ GeV) |
| $\sigma(W^\pm Z)$ | $= 18.0 \pm 1.3$ pb ($66 < M_Z < 116$ GeV) |
| $\sigma(W^+Z)$ | $= 11.9 \pm 0.8$ pb ($M_Z > 60$ GeV) |
| $\sigma(W^-Z)$ | $= 6.66 \pm 0.47$ pb ($M_Z > 60$ GeV) |
| $\sigma(W^\pm Z)$ | $= 18.5 \pm 1.3$ pb ($M_Z > 60$ GeV) |
| $\sigma(ZZ)$ | $= 5.64 \pm 0.28$ pb ($66 < M_Z < 116$ GeV) |
| $\sigma(ZZ)$ | $= 5.96 \pm 0.30$ pb ($M_Z > 60$ GeV) |
| $\sigma(ZZ)$ | $= 9.23 \pm 0.46$ pb ($M_Z > 12$ GeV) |

TABLE XX: Summary of $q\bar{q}'$ and q/g initiated diboson cross sections calculated up to NLO QCD. Note that the Z above includes both vector boson Z and virtual photon γ^* contributions. Cross sections for different $Z(\gamma^*)$ mass ranges can be obtained from Table XIV.

It should be cautioned though there are significant uncertainties on WW and ZZ cross sections due to higher order contributions from $gg \rightarrow WW$ and $gg \rightarrow ZZ$ as discussed in Section III D. We opted not to combine $qq/qg \rightarrow WW/ZZ$ with $gg \rightarrow WW/ZZ$ cross sections as these processes are likely to be separately evaluated in Monte Carlo simulations.

F. Cross sections for different values of \sqrt{s}

Tables XXI and XXII show the inclusive diboson cross sections as a function of the center-of-mass energy, for $p\bar{p}$ and pp colliders respectively. Results are obtained with MCFM program with MSTW2008NLO PDF set. No cuts

have been applied on W bosons, while WZ and ZZ results are given for two different cuts on the Z invariant mass, at 12 and 60 GeV. These results are graphically illustrated in Fig. 7.

| \sqrt{s} (TeV) | WW | WZ | | ZZ | |
|---------------------|-------|------------------------|------------------------|------------------------|------------------------|
| | | $M_Z > 12 \text{ GeV}$ | $M_Z > 60 \text{ GeV}$ | $M_Z > 12 \text{ GeV}$ | $M_Z > 60 \text{ GeV}$ |
| 0.4 | 0.071 | 0.159 | 0.004 | 0.088 | 0.003 |
| 0.6 | 0.664 | 0.464 | 0.082 | 0.258 | 0.052 |
| 0.63 | 0.808 | 0.526 | 0.107 | 0.291 | 0.065 |
| 0.8 | 1.83 | 0.945 | 0.314 | 0.508 | 0.170 |
| 1.0 | 3.32 | 1.58 | 0.688 | 0.804 | 0.337 |
| 1.2 | 4.96 | 2.31 | 1.16 | 1.12 | 0.532 |
| 1.4 | 6.66 | 3.12 | 1.71 | 1.45 | 0.743 |
| 1.6 | 8.39 | 3.98 | 2.30 | 1.78 | 0.961 |
| 1.8 | 10.11 | 4.85 | 2.92 | 2.12 | 1.18 |
| 1.96 | 11.49 | 5.60 | 3.44 | 2.39 | 1.36 |
| 2.0 | 11.84 | 5.76 | 3.56 | 2.46 | 1.41 |
| 3.0 | 20.39 | 10.62 | 7.03 | 4.14 | 2.56 |
| 4.0 | 29.03 | 15.73 | 10.74 | 5.83 | 3.73 |
| 5.0 | 37.90 | 21.16 | 14.65 | 7.56 | 4.94 |
| 6.0 | 47.06 | 26.77 | 18.75 | 9.38 | 6.18 |
| 7.0 | 56.43 | 32.57 | 23.02 | 11.21 | 7.47 |
| 8.0 | 66.14 | 38.51 | 27.44 | 13.05 | 8.79 |
| 9.0 | 75.97 | 44.65 | 31.98 | 14.96 | 10.13 |
| 10.0 | 86.16 | 51.05 | 36.66 | 16.95 | 11.51 |
| 11.0 | 96.47 | 57.10 | 41.47 | 18.86 | 12.92 |
| 12.0 | 106.8 | 63.66 | 46.35 | 20.90 | 14.35 |
| 13.0 | 117.5 | 70.14 | 51.33 | 22.89 | 15.82 |
| 14.0 | 128.3 | 77.33 | 56.45 | 24.95 | 17.25 |
| 15.0 | 139.0 | 83.94 | 61.59 | 26.91 | 18.75 |

TABLE XXI: Diboson inclusive cross section in pb calculated at NLO for different center-of-mass energies of $p\bar{p}$ collisions. They are obtained using the MCFM program with MSTW2008NLO PDF set. No cuts are applied on W bosons. ZZ results are given for two different cuts on the Z invariant mass, at 12 and 60 GeV.

| \sqrt{s} (TeV) | WW | $M_Z > 12 \text{ GeV}$ | | | | $M_Z > 60 \text{ GeV}$ | | | |
|---------------------|-------|------------------------|--------|-----------|-------|------------------------|--------|-----------|-------|
| | | W^+Z | W^-Z | $W^\pm Z$ | ZZ | W^+Z | W^-Z | $W^\pm Z$ | ZZ |
| 0.4 | 0.002 | 0.030 | 0.010 | 0.040 | 0.017 | | | | |
| 0.6 | 0.052 | 0.114 | 0.041 | 0.154 | 0.054 | 0.005 | 0.002 | 0.008 | 0.003 |
| 0.63 | 0.069 | 0.131 | 0.047 | 0.178 | 0.062 | 0.008 | 0.003 | 0.011 | 0.005 |
| 0.8 | 0.236 | 0.252 | 0.097 | 0.350 | 0.122 | 0.038 | 0.012 | 0.050 | 0.020 |
| 1.0 | 0.596 | 0.452 | 0.181 | 0.633 | 0.226 | 0.115 | 0.037 | 0.152 | 0.058 |
| 1.2 | 1.13 | 0.710 | 0.293 | 1.00 | 0.361 | 0.241 | 0.080 | 0.321 | 0.120 |
| 1.4 | 1.82 | 1.02 | 0.431 | 1.45 | 0.528 | 0.412 | 0.141 | 0.552 | 0.203 |
| 1.6 | 2.65 | 1.38 | 0.594 | 2.16 | 0.715 | 0.621 | 0.221 | 0.841 | 0.305 |
| 1.8 | 3.59 | 1.76 | 0.780 | 2.54 | 0.925 | 0.861 | 0.318 | 1.18 | 0.424 |
| 1.96 | 4.42 | 2.09 | 0.947 | 3.04 | 1.11 | 1.07 | 0.408 | 1.48 | 0.530 |
| 2.0 | 4.62 | 2.18 | 0.991 | 3.18 | 1.16 | 1.13 | 0.433 | 1.56 | 0.558 |
| 3.0 | 10.93 | 4.63 | 2.30 | 6.93 | 2.48 | 2.78 | 1.22 | 4.00 | 1.38 |
| 4.0 | 18.46 | 7.47 | 3.95 | 11.42 | 4.02 | 4.76 | 2.31 | 7.07 | 2.38 |
| 5.0 | 26.75 | 10.58 | 5.86 | 16.43 | 5.70 | 6.98 | 3.60 | 10.58 | 3.50 |
| 6.0 | 35.66 | 13.83 | 7.96 | 21.79 | 7.44 | 9.35 | 5.06 | 14.42 | 4.69 |
| 7.0 | 44.92 | 17.21 | 10.18 | 27.39 | 9.23 | 11.87 | 6.66 | 18.53 | 5.96 |
| 8.0 | 54.71 | 20.72 | 12.60 | 33.31 | 11.17 | 14.45 | 8.38 | 22.83 | 7.27 |
| 9.0 | 64.65 | 24.28 | 15.09 | 39.37 | 13.04 | 17.16 | 10.19 | 27.35 | 8.62 |
| 10.0 | 74.93 | 27.93 | 17.72 | 45.64 | 15.02 | 19.94 | 12.08 | 32.02 | 10.01 |
| 11.0 | 85.30 | 31.68 | 20.38 | 52.06 | 16.99 | 22.76 | 14.04 | 36.80 | 11.42 |
| 12.0 | 95.95 | 35.44 | 23.08 | 58.52 | 18.96 | 25.64 | 16.08 | 41.72 | 12.86 |
| 13.0 | 106.8 | 39.25 | 25.89 | 65.14 | 21.04 | 28.56 | 18.17 | 46.72 | 14.34 |
| 14.0 | 117.7 | 43.13 | 28.72 | 71.85 | 23.11 | 31.55 | 20.30 | 51.85 | 15.81 |
| 15.0 | 128.7 | 47.13 | 31.66 | 78.80 | 25.17 | 34.54 | 22.49 | 57.03 | 17.34 |

TABLE XXII: Diboson inclusive cross section in pb calculated at NLO for different center-of-mass energies of pp collisions. They are obtained using the MCFM program with MSTW2008NLO PDF set. No cuts are applied on W bosons, while WZ and ZZ results are given for two different cuts on the Z invariant mass, at 12 and 60 GeV.

IV. SUMMARY

Total inclusive cross sections in pp collisions at $\sqrt{s} = 7 \text{ TeV}$ for single W and Z bosons up to NNLO and for dibosons up to NLO are presented. Their dependences on factorization and renormalization scales, parton density functions as well as on the strong coupling constant are studied from which total theoretical uncertainties are estimated. Production cross sections for other center-of-mass energies in both pp and $p\bar{p}$ are also included.

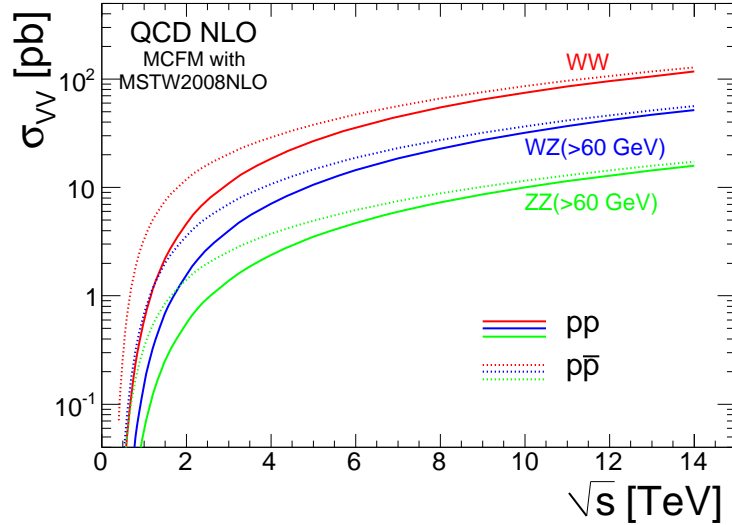


FIG. 7: Diboson inclusive cross sections with NLO in QCD corrections as functions of center-of-mass energies in pp and $p\bar{p}$ collisions.

V. ACKNOWLEDGEMENT

We wish to thank Mohamed Aharrouche, Daniel Froidevaux, Karl Jacob, Aleandro Nisati, Jonas Strandberg and Manuella Vinciter for fruitful discussions and encouragement. We would like to express our gratitude to John Campbell, Nikolas Kauer, Frank Petriello and Stefano Frixione for their assistance in carrying out this study.

-
- [1] ATLAS Collaboration, *Measurement of the $W \rightarrow \ell\nu$ production cross-section and observation of $Z \rightarrow \ell\ell$ production in pp collisions at $\sqrt{s} = 7$ TeV with the ATLAS detector*, ATLAS-CONF-2010-051 (2010);
ATLAS Collaboration, *Measurement of the $Z \rightarrow \ell\ell$ production cross section in pp collisions at $\sqrt{s} = 7$ TeV with the ATLAS detector*, ATLAS-CONF-2010-076 (2010);
ATLAS Collaboration, *Supporting Document: Total inclusive W and Z boson cross-section measurements, cross-section ratios and combinations in the electron and muon decay channels at 7 TeV based on 300 nb^{-1}* , ATLAS-COM-PHYS-2010-703 (2010).
 - [2] G. Aad et al. (ATLAS Collaboration), *Expected Performance of the ATLAS Experiment: Detector, Trigger and Physics*, CERN-OPEN-2008-020, Geneva, Switzerland, 2008; also as [arXiv:0901.0512](#) (2009);
D. Rebuzzi et al., *Cross-sections for Standard Model processes for the ATLAS CSC studies*, ATLAS Note ATL-PHYS-INT-2009-003;
K. Assamagan et al., *Production Cross Section of the Higgs Boson and Other Standard Model Processes in pp Collisions at Different Center-of-Mass Energies*, ATLAS Note ATL-COM-PHYS-2009-051;
H. Liu et al., *Production Cross Sections of Standard Model Processes in pp Collisions at $\sqrt{s} = 10$ TeV and Their Dependences on QCD Scales*, ATLAS Note ATL-COM-PHYS-2009-242.
 - [3] S. Frixione and B. R. Webber, "Matching NLO QCD computations and parton shower simulations", JHEP 0206 (2002) 029 [[hep-ph/0204244](#)].
 - [4] G. Corcella et al., *HERWIG 6.5*, JHEP 0101 (2001) 010 [[hep-ph/0011363](#)], *ibid* [hep-ph/0210213](#).
 - [5] J. M. Campbell and R. K. Ellis, *An update on vector boson pair production at hadron colliders*, Phys. Rev. D60, 113006 (1999) [[hep-ph/9905386](#)].
 - [6] C. Anastasiou, L. Dixon, K. Melnikov and F. Petriello, Phys. Rev. D **69**, 094008 (2004) [[hep-ph/0312266](#)].
 - [7] R. Hamberg, W. L. van Neerven and T. Matsuura, Nucl. Phys. B **359** (1991) 343 [Erratum-*ibid.* B **644** (2002) 403]. Original program code available at <http://www.lorentz.leidenuniv.nl/~neerven/DECEASED>.
 - [8] M.R. Whalley, D. Bourilkov, and R.C. Group, *The Les Houches Accord PDFs (LHAPDF) and LHAGLUE*, 2005 [[hep-ph/0508110](#)].
 - [9] T. Binoth, M. Ciccolini, N. Kauer, and M. Kramer, JHEP 12 (2006) 046.
 - [10] T. Binoth, N. Kauer and P. Mertsch, *Gluon-induced QCD corrections to $pp \rightarrow ZZ \rightarrow \ell\bar{\ell}\ell'\bar{\ell}'$* , [arXiv:0807.0024](#).
 - [11] Standard model input parameter values for **mc09** Monte Carlo production:
<https://twiki.cern.ch/twiki/bin/view/AtlasProtected/McProductionCommonParameters>.
 - [12] W.-M. Yao et al. (Particle Data Group), *The Review of Particle Physics*, 2007 Edition, J. Phys. G**33**, 1 (2006).

- [13] H.L. Lai *et al.*, E. Phys. J. **C12**, 375 (2000); J. Pumplin *et al.*, JHEP **0207**, 012 (2002); P.M. Nadolsky *et al.*, Phys. Rev. D **78**, 013004 (2008) [arXiv:0802.0007].
- [14] H. L. Lai, M. Guzzi, J. Huston, Z. Li, P. M. Nadolsky, J. Pumplin and C. P. Yuan, arXiv:1007.2241 [hep-ph].
- [15] A.D. Martin, W.J. Stirling, R.S. Thorne and G. Watt, Phys. Lett. B **652**, 292 (2007); *ibid* arXiv:0901.0002 (2009);
- [16] F. D. Aaron *et al.* [H1 Collaboration and ZEUS Collaboration], JHEP **1001** (2010) 109 [arXiv:0911.0884 [hep-ex]].
- [17] H1 and ZEUS Collaborations, H1prelim-10-044/ZEUS-prel-10-008 (2010), Contribution 318 at DIS10, XVIII International Workshop on Deep Inelastic Scattering, talk by V. Radescu,
<http://indico.cern.ch/contributionDisplay.py?sessionId=4&contribId=318&confId=86184>.
- [18] https://www.desy.de/h1zeus/combined_results/index.php?do=proton_structure
- [19] S. Alekhin, J. Blumlein, S. Klein and S. Moch, Phys. Rev. D **81**, 014032 (2010) [arXiv:0908.2766 [hep-ph]].
- [20] M. Aharrouché *et al.*, “Double differential Z, W cross sections and their ratios in the electron channels”, ATLAS Note ATL-COM-PHYS-2010-325 (page 132).
- [21] A.D. Martin, W.J. Stirling, R.S. Thorne and G. Watt, Eur. Phys. J. C **64**, 653 (2009) [arXiv:0905.3531 [hep-ph]].
- [22] D. A. Dicus, C. Kao and W. W. Repko, Phys. D36, 1570 (1987).
- [23] W. W. N. Glover and J.J. van der Bij, Nucl. Phys. B321, 561 (1989).
- [24] T. Matsuura and J. J. van der Bij, Z. Phys. C51, 259 (1991).
- [25] C. Zecher, T. Matsuura and J. J. van der Bij, Z. Phys. C64, 219 (1994), also as hep-ph/9404295.
- [26] T. Binoth, N. Kauer and P. Mertsch, arXiv:0807.0024 (2008).
- [27] J. M. Campbell *et al.*, “Normalizing Weak Boson Pair Production at the Large Hadron Collider”, Phys. Rev. D80, 054023 (2009) [arXiv:0906.2500 [he-ph]].
- [28] S. Frixione, the off-shell effect is currently under implementation for WZ , private communication.

APPENDIX A: FEWZ

The following text is an example of `input.txt` for calculating NNLO $Z/\gamma^* \rightarrow \ell\ell$ cross section in pp collisions at a center-of-mass energy $\sqrt{s} = 7$ TeV with the MSTW2008NNLO PDF set. The $M_{\ell\ell}$ range is set in source code `constraint.F`.

```

CMS collision energy (GeV)      = ' 7000d0
=====
'Factorization scale (GeV)     = ' 91.1876d0
'Renormalization scale (GeV)  = ' 91.1876d0
=====
'Z production (4=LHC,5=TEV)   = ' 4
=====
'Alpha QED                    = ' 0.0075563d0
'Fermi constant (1/GeV^2)     = ' 0.0000116637d0
=====
'W mass (GeV)                 = ' 80.403d0
'Z mass (GeV)                 = ' 91.1876d0
'Z width (GeV)                = ' 2.4952d0
'W width (GeV)                = ' 2.0910d0
'Z->ll partial width          = ' 0.08398d0
'W->lv partial width          = ' 0.22629d0
'sin^2(theta)                 = ' 0.22255d0
'up quark charge              = ' 0.6666667d0
'down quark charge            = ' -0.3333333d0
'lepton charge                = ' -1d0
'up quark vector coupling     = ' 0.4065d0
'down quark vector coupling   = ' -0.7033d0
'lepton vector coupling       = ' -0.1098d0
'up quark axial coupling      = ' -1d0
'down quark axial coupling    = ' 1d0
'lepton axial coupling        = ' 1d0
=====
'Perturb. Order (0=LO, 1=NLO, 2=NNLO) = ' 2
'Z pole focus (0=Yes, 1=No)      = ' 0
'Upper M limit (for non-Zpole) = ' 1000.0d0
=====
'PDF set =                      ' 'MSTW2008NNLO'
=====
'Output File                    = ' 'Output.dat'

```

APPENDIX B: MCFM

In MCFM, the parameter `.zerowidth.` gives the possibility to choose on-shell or off-shell bosons. The option “zerowidth = .true.” puts W and Z bosons exactly on-shell. When the option with “zerowidth = .false.” is selected, the generated events correspond to the corresponding Breit-Wigner distributions, with the appropriate width. When integrated over all the mass range, this gives back (to 1% level of accuracy) the same result as “zerowidth = .true.”

The following is an example of `input.DAT` for calculating NLO $Z/\gamma^* \rightarrow \ell\ell$ cross section in pp collisions at $\sqrt{s} = 7$ TeV with the MSTW2008NLO PDF set. The dilepton mass range is set to be between 66 – 116 GeV (parameters `m34min` and `m34max`). Since the parameter `removebr` is set to be `.true.`, the program returns the total Z/γ^* cross section.

```
'5.8'                [file version number]

[Flags to specify the mode in which MCFM is run]
.false.              [evtgen]
.false.              [creatent]
.false.              [skipnt]
.false.              [dswhisto]

[General options to specify the process and execution]
31                   [nproc]
'tota'               [part 'lord','real' or 'virt','tota']
'test'               ['runstring']
7000d0               [sqrts in GeV]
+1                   [ih1 =1 for proton and -1 for antiproton]
+1                   [ih2 =1 for proton and -1 for antiproton]
120d0                [hmass]
-1d0                 [scale:QCD scale choice]
-1d0                 [facscale:QCD fac_scale choice]
.false.              [dynamicscale]
.false.              [zerowidth]
.true.               [removebr]
10                   [itmx1, number of iterations for pre-conditioning]
20000                [ncall1]
10                   [itmx2, number of iterations for final run]
100000               [ncall2]
1089                 [ij]
.false.              [dryrun]
.false.              [Qflag]
.true.               [Gflag]

[Heavy quark masses]
172.5d0              [top mass]
4.2d0                [bottom mass]
1.29d0               [charm mass]

[Pdf selection]
'mstw8n1'            [pdlabel]
4                    [NGROUP, see PDFLIB]
00                   [NSET - see PDFLIB]
MSTW2008nlo90cl.LHgrid [LHAPDF group]
-1                   [LHAPDF set]

[Jet definition and event cuts]
66d0                 [m34min]
116d0                [m34max]
0d0                  [m56min]
10000d0              [m56max]
.true.               [inclusive]
'ktal'               [algorithm]
```

```

0d0      [ptjet_min]
0d0      [|etajet|_min]
99d0     [|etajet|_max]
0.4d0    [Rcut_jet]
.false.  [makecuts]
0d0      [ptlepton_min]
99d0     [|etalepton|_max]
0d0      [ptmin_missing]
0d0      [ptlepton(2nd+)_min]
99d0     [|etalepton(2nd+)|_max]
0.7d0    [R(jet,lept)_min]
0.7d0    [R(lept,lept)_min]
0d0      [Delta_eta(jet,jet)_min]
.false.  [jets_opphem]
0        [lepbtwnjets_scheme]
20d0     [ptmin_bjet]
2.5d0    [etamax_bjet]
6.5d0    [ptmin_photon]
2.5d0    [etamax_photon]
0.7d0    [cone_photon]
1d0      [cone_ptcut]

```

[Anomalous couplings of the W and Z]

```

0.0d0    [Delta_g1(Z)]
0.0d0    [Delta_K(Z)]
0.0d0    [Delta_K(gamma)]
0.0d0    [Lambda(Z)]
0.0d0    [Lambda(gamma)]
2.0d0    [Form-factor scale, in TeV]

```

[How to resume/save a run]

```

.false.  [readin]
.false.  [writeout]
''       [ingridfile]
''       [outgridfile]

```

[Technical parameters that should not normally be changed]

```

.false.  [debug]
.true.   [verbose]
.false.  [new_pspace]
.false.  [virtonly]
.false.  [realonly]
.true.   [spira]
.false.  [noglu]
.false.  [ggonly]
.false.  [gqonly]
.false.  [vanillafiles]
1        [nmin]
2        [nmax]
.true.   [clustering]
.false.  [realwt]
0        [colourchoice]
1d-2     [rtsmin]
1d-4     [cutoff]
1d0      [a11]
1d0      [a12]
1d0      [a13]
1d0      [a14]

```

APPENDIX C: MC@NLO

Single boson production processes are treated in MC@NLO as dilepton production processes and the inclusive cross section is obtained by integrating on the lepton degrees of freedom. The program provide, for each given process, the branching ratio of the vector boson in the given final state, and these have been used here to provide the results for the Z or W inclusive cross sections. The leptonic cross section divided by the given branching ratio concides *exactly* with the vector boson production cross section only in the $\Gamma_Z \rightarrow 0$ limit.

Process IPROC = -1350 ($Z/\gamma^*(\rightarrow l\bar{l}) + X$), includes interference and in general the Z boson is not on shell. Process -1397 allows to calculate the inclusive cross section with the Z boson on shell. In this case the spin correlation between lepton is lost, but this does not affect the inclusive result, which is discussed here. For W mediated processes, IPROC -1460 (W^+) and -1470 (W^-) have been selected, to be compared with IPROC -1497 (W^+) and -1498 (W^-), in which the W boson is on-mass shell.

The following is an example of MCatNLO.inputs for calculating NLO ZZ cross section in pp collisions at $\sqrt{s} = 7$ TeV with the MSTW2008NLO PDF set. The dilepton mass range is set to be between 70–110 GeV (parameters V1MASSINF and V1MASSSUP, and similar for V2). In this input file configuration, the program returns the total ZZ cross section and the set of 500000 hard events.

```
# This is a bash script that compiles and runs all of the MC@NLO codes.
# On your system, you need:
#
#   bash shell      AND      gmake
#
# which are rather standard (ask your system manager if they are not
# available).
#
# HOW TO USE THIS SCRIPT:
# Look for "physical parameters" and "other input parameters" in
# in this file; they control all the inputs for the MC@NLO codes.
# After having modified them to suit your needs, execute this
# file from a bash shell. Notice that the only command in this
# file is
#   runMCatNLO
# which is what you need in order to obtain MC@NLO results. Other
# commands are available: see at the bottom of this file for a
# list of them. In this version, they are all commented out;
# uncomment them if you need them.
#
# WHAT THE USER MUST DO PRIOR TO RUNNING
# The files
#   mcatnlo_hwdriver.f   mcatnlo_hwlhin.f
# must be edited in order to insert the 'INCLUDE HERWIGXX.INC' command
# relevant to the version of HERWIG your are going to use. The file(s)
#   mcatnlo_hwanXXX.f
# contain sample analysis routines, and must be edited for the same reason.
# Notice, however, that these analysis routines are provided here to furnish
# a ready-to-run package, but they are identical to standard HERWIG analysis
# routines, and should therefore be replaced with your analysis routines.
# In this case, you will simply set the variable HWUTI (in this file) equal
# to the list of object files you need in your routines.
# Finally, the variable HERWIGVER below must be set equal to the name
# of your preferred version of HERWIG (matching the one whose common
# blocks are included in the files above)
#
#!/bin/bash
#
#
# physical parameters
#
#
```

```

# CM energy
ECM=7000
# renormalization scale factor
FREN=1
# factorization scale factor
FFACT=1
# mass of the heavy quark (bottom for IPROC=-1705, top otherwise, including
# Higgs production)
HVQMASS=172.5
# width of the top. A negative entry will force the code to compute the width
# at the LO in the SM, in ttbar and single top production and when the
# tops decay
TWIDTH=1.320
# W mass
WMASS=80.403
# W width. A negative entry will force the code to compute the width
# at the LO in the SM, in single top production (Wt channel) when the
# top and W decay, and in WW production when the W's decay
WWIDTH=2.0910
# Z mass
ZMASS=91.1876
# Z width
ZWIDTH=2.4952
# branching ratio for Sum_j (top -> l nu_l b_j), with b_j any down-type
# quark, and l a given lepton species. Lepton universality is assumed
BRTOPTOLEP=0.1111
# branching ratio for Sum_ij (top -> u d_i b_j), with d_i and b_j any
# down-type quarks. Flavour universality is assumed
BRTOPTOHAD=0.3333
# branching ratio for W -> l nu_l, with l a given lepton species.
# Lepton universality is assumed
BRWTOLEP=0.108
# branching ratio for Sum_i (W -> u d_i), with d_i any
# down-type quarks. Flavour universality is assumed
BRWTOHAD=0.3333
# Higgs mass
HGGMASS=120
# Higgs width: MC@NLO does not compute the SM width associated with the
# mass set in HGGMASS. The user must set the width by hand
HGGWIDTH=0.0049
# In the computation of the Higgs cross section at the Born level:
# IBORNHGG=1 --> exact M_top dependence, IBORNHGG=2 --> M_top -> infinity
IBORNHGG=1
# When the mass of a particle P is distributed according to Breit-Wigner
# (which happens in production for the Drell Yan process if P is a W, Z,
# or photon, and in decay if P is a top, a vector boson, or a Higgs),
# the mass range is (if PGAMMAX>0)
#   MO_P - PGAMMAX * WIDTH < M_P < MO_P + PGAMMAX * WIDTH
# with MO_P the pole mass of P, and WIDTH its width. If PGAMMAX<0 then
#   PMASSINF < M_P < PMASSSUP
# Valid shell variables correspond to
#   P = V1, V2, T1, T2, H
# for vector boson, top, and Higgs respectively. In the case of top decay,
# the shell variables with prefix Vj are relevant to the W's emerging from
# the decay of the top whose shell variables have prefix Tj.
# When there is only one vector boson or one top in the final state,
# the relevant shell variables have prefix V1 or T1. In the case of
# vector boson pair production, the prefixes (V1,V2) correspond to (W+,W-),

```



```

# (Z,Z), (W+,Z), and (W-,Z) for IPROC=-2850, -2860, -2870, and 2880
# respectively. In the case of ttbar production, (T1,T2) correspond
# to (t,tbar), and (V1,V2) to (W+,W-) emerging from (t,tbar) decays.
# In the case of tW- production, T1 and V2 correspond to t and W- produced
# in the hard reaction respectively (in version 3.4, off-shell effects are
# however not implemented yet), and V1 to the W+ emerging from the t decay
V1GAMMAX=-1
V1MASSINF=70
V1MASSSUP=110
V2GAMMAX=-1
V2MASSINF=70
V2MASSSUP=110
T1GAMMAX=30
T1MASSINF=0
T1MASSSUP=0
T2GAMMAX=30
T2MASSINF=0
T2MASSSUP=0
HGAMMAX=30
HMASSINF=0
HMASSSUP=0
# quark and gluon masses (used only by HERWIG)
UMASS=0.32
DMASS=0.32
SMASS=0.5
CMASS=1.29
BMASS=4.2
GMASS=0.75
# absolute values of the CKM matrix elements; used for single-top production
# and subsequent top decay, and for top decay in ttbar production.
# Set VUD=VUS=VUB=0 to use the defaults in the code
VUD=0.9738
VUS=0.2272
VUB=0.0040
VCD=0.2271
VCS=0.9730
VCB=0.0422
VTD=0.0081
VTS=0.0416
VTB=0.9991
# Set AEMRUN=YES to use running alpha_em, AEMRUN=NO to use the Thomson value
AEMRUN=YES
# process number; MC@NLO process codes are negative. A positive process
# code may be used (executing runMC) to run standard HERWIG
IPROC=-2860
# vector boson code: IVCODE=-1,0,1 for W^-, Z, and W^+ respectively.
# This variable is only used in WH and ZH production
IVCODE=1
# IL1CODE determines the identities of decay products of tops or
# vector bosons, when spin correlations are included.
# Set IL1CODE=7 for undecayed vector bosons or tops.
# IL1CODE is relevant to WH, ZH, single-top, ttbar, and vector boson
# pair production; in the latter two cases, and in Wt production, the
# variable IL2CODE is also needed. See the manual for a list of valid
# values for IL1CODE and IL2CODE. In the case of VV, ttbar and tW
# production, (IL1CODE,IL2CODE) control the decays of (t,tbar), (t,W),
# (W+,W-), (Z,Z), (W+,Z), and (W-,Z) for IPROC=-1706, -2030, -2850,
# -2860, -2870, and 2880 respectively

```

```

IL1CODE=7
IL2CODE=7
# type of top decay: set TOPDECAY=Wb to allow only t->Wb decays; set
# TOPDECAY=ALL to allow all t->W+down-type-quark decays. In the latter
# case, the flavour of the down quark is determined using the CKM
# matrix elements entered here
TOPDECAY=Wb
# set WTTYPE=REMOVAL to perform the computation of the Wt cross section in
# the Diagram Removal (DR) scheme. Set WTTYPE=SUBTRACTION to use the
# Diagram Subtraction (DS) scheme. See JHEP 0807:029,2008 [arXiv:0805.3067]
WTTYPE=REMOVAL
# ptveto value, used for factorization scale computation if FFACT<0, and
# for renormalization scale computation if FREN<0. Effective only for Wt
PTVETO=50
# incoming left beam
PART1=P
# incoming right beam
PART2=P
# PDF group name; unused when linked to LHAPDF
PDFGROUP=LHAPDF
# PDF set number; use LHAGLUE conventions when linked to LHAPDF
PDFSET=21100
# Lambda_5, used in NLO computations. A negative entry returns the value
# resulting from PDF fit.
# WARNING: negative entries may lead to inconsistent results when using
# PDFLIB or LHAPDF: use a positive entry when in doubt
LAMBDAFIVE=-1
# Scheme
SCHEMEOFPDF=MS
# Lambda_5, used by HERWIG. A negative entry returns the HERWIG default value
LAMBDAHERW=-1
#
#
# other input parameters
#
#
# prefix for BASES files; relevant to the integration step
FPREFIX=ZZ
# prefix for event file; relevant to the event generation step
EVPREFIX=ZZ
# prefix for the NLO and MC executables
EXEPREFIX=ZZ
# number of events; set it to 0 to skip the event generation step
NEVENTS=500000
# 0 for weights=+1/-1, 1 for weights whose sum is the total rate
WGTTYPE=1
# seed for random numbers in the generation of events. 0 is default
RNDEVSEED=0
# set BASES=ON to perform integration, =OFF to skip the integration step
BASES=ON
# set PDFLIBRARY=THISLIB, =PDFLIB, or =LHAPDF to obtain PDFs from our
# private PDF library, from PDFLIB or from LHAPDF respectively
PDFLIBRARY=LHAPDF
# set HERPDF=DEFAULT to use HERWIG default PDFs, HERPDF=EXTPDF to use
# the same PDFs as used in the NLO; the setting of this parameter is
# independent of the setting of PDFLIBRARY
HERPDF=DEFAULT
# the variable HWPATH must be set equal to the name of directory

```

```

# which contains the version of HERWIG the user wants to link
# to his code
HWPATH="/home/frixione/CERN/mcatnlo/test/"
# prepend this string to prefixes to avoid storage problems
# leave blank to store event and data files in the running directory
SCRTCH=
# set the following variable equal to the list of object files that
# you need when using HERWIG (for analysis purposes, for example)
HWUTI="mcatnlo_hwantop.o mcatnlo_hbook.o"
# set the following variable equal to the name of the version of
# HERWIG that you use
HERWIGVER="herwig6510.o"
# set the following variable equal to the name of the directory where
# the PDF grid files are stored. Effective only if PDFLIBRARY=THISLIB
PDFPATH="/home/frixione/PDFgrids/"
# set the following variable equal to the name of the directory where
# the local version of LHAPDF is installed. We assume that the library,
# PDF sets, and configuration script are located in lib/,
# share/lhapdf/PDFsets/, and bin/ respectively
LHAPATH="/user/rebuzzi/HAWK/LHAPDF"
# set LHAOFL=FREEZE to freeze PDFs from LHAPDF at the boundaries,
# =EXTRAPOLATE otherwise. This variable is related to LHAPARM(18)
LHAOFL=FREEZE
# set the following variable equal to the names of the libraries which
# need be linked. Library names are separated by white spaces.
# Note: LHAPDF is a special case, and must not be included here
EXTRALIBS=
# set the following variable equal to the paths to the libraries which
# need be linked. Library paths are separated by white spaces.
# Note: LHAPDF is a special case, and must not be included here
EXTRAPATHS=
# set the following variable equal to the paths to the directories which
# contain header files needed by C++ files. Directory names are separated
# by white spaces
INCLUDEPATHS=
#
#
#
# NOW LOAD THE SCRIPTS: DO NOT REMOVE THESE LINES
thisdir='pwd'
. $thisdir/MCatNLO_dyn.Script
#
#
#
#
#
#
# HERE, WRITE THE NAME OF THE SHELL FUNCTION THAT YOU NEED TO
# EXECUTE CHOOSING AMONG (ONLY ONE AT A TIME):
#
#   runMCatNLO  runNLO  runMC  compileNLO  compileMC
#
# THEIR MEANINGS ARE DESCRIBED IN WHAT FOLLOWS
#
#
# the following compiles and runs both the NLO and MC codes
# runMCatNLO
# the following compiles and runs the NLO only (thus, the event file

```

```
# is written, but not read by HERWIG)
runNLO
# the following compiles and runs the MC only (thus, the event file must
# be already present, otherwise the program crashes)
# runMC
# the following compiles NLO code
# compileNLO
# the following compiles MC code
# compileMC
# runMCatNLO
```